Numer. Math. (2014) 127:715–749
DOI 10.1007/s00211-013-0601-1

Numerische Mathematik

Convergence analysis for a conformal discretization of a model for precipitation and dissolution in porous media

K. Kumar · I. S. Pop · F. A. Radu

Received: 04 April 2012 / Revised: 11 March 2013 / Published online: 5 December 2013

Abstract In this paper we discuss the numerical analysis of an upscaled (core scale) model describing the transport, precipitation and dissolution of solutes in a porous medium. The particularity lies in the modeling of the reaction term, especially the dissolution term, which has a multivalued character. We consider the weak formulation for the upscaled equation and provide rigorous stability and convergence results for both the semi-discrete (time discretization) and the fully discrete schemes. In doing so, compactness arguments are employed.

Mathematics Subject Classification 35A35 · 65L60 · 65J20

1 Introduction

In this paper we consider a model for the reactive flow in a porous medium, where the ions/solutes are being transported through the combined process of convection and diffusion. Such models are encountered in many real-life applications, like the spreading of chemical and the resulting ground water contamination (see [1] and references therein), biological applications such as tissue and bone formation, pharmaceutical applications [2], or the operation of solid state batteries. Of particular interest are the

K. Kumar
Center for Subsurface Modeling, The University of Texas at Austin, Austin, USA

I. S. Pop (✉)
Department of Mathematics and Computer Science, Eindhoven University of Technology, Eindhoven, The Netherlands
e-mail: i.pop@tue.nl

I. S. Pop · F. A. Radu
Institute of Mathematics, University of Bergen, Bergen, Norway

reactive processes, where precipitation and dissolution fronts develop as a result of reactions (see [3–5] and references therein). In a related context, [6] discusses the presence of stiff dissolution fronts involving the applications in the nuclear waste disposal.

Here we concentrate on a macroscale (upscaled) model, meaning that the model is defined at the Darcy scale. Therefore no distinction is made between the solid grains and the pore space, and the equations are defined everywhere in the domain of interest. The interesting aspect of the flow is the description of reactions taking place which have a particular structure. These reactions model the precipitation and dissolution processes taking place due to the interactions of ions (cations and anions). The reactions lead to the formation of crystals which are immobile species. Since the model is considered at macroscale, both the crystals and the ions are defined everywhere. We take the model which was first proposed in [7] and then followed in a series of papers [8–10]. In [11], the corresponding pore scale model was presented. Further, the upscaled model is derived rigorously in a simplified situation of a 2D strip.

The dissolution and precipitation models mentioned above are assuming a constant-in-time pore structure, i.e. no changes in the pore space is encountered due to precipitation or dissolution. Alternatively, one can consider the situation when the precipitate is viewed as a layer attached to the pore walls, having a variable in time thickness. This leads to models involving free boundaries at the pore scale, as analyzed in [12], where the existence and uniqueness of a solution and the existence of a free boundary separating fluid from precipitate is proved in one spatial dimension (see also [13] for the analysis of a similar, one-dimensional model encountered in concrete carbonation). The formal upscaling (from the pore scale to the Darcy scale) of such models in a simple pore is discussed in [14,15]; for the case of rough boundaries we refer to [16], whereas for applications related to biofilm growth in porous media or drug release from collagen matrices we refer to [17,18].

Our main goal here is to provide the convergence of a conforming FEM discretization for an upscaled model for dissolution and precipitation in porous media, involving a multi-valued dissolution rate. These results are announced in [19]. Before discussing the details, we briefly review some of the numerical work that is related to the present context. Conformal FEM schemes for reactive porous media flow models are discussed in [20,21], where non-Lipschitz, but Hölder continuous rates are considered. Similarly, for Hölder continuous rates (including equilibrium and non-equilibrium cases) mixed FEM methods are analyzed rigorously in [22,23], whereas [24] provides error estimates for the coupled system describing unsaturated flow and reactive transport (see also [25] for a model appearing in concrete carbonation and including a concentration-dependent porosity, and [26] for a numerical investigation of the carbonation front in concrete). In the cases mentioned before, the continuity of the reaction rates allows obtaining error estimates. Further, for continuously differentiable rates, the convergence of (adaptive) finite volume discretizations is studied in [27,28]; see also [29] for the convergence of a finite volume discretization of a copper-leaching model. In a similar framework, discontinuous Galerkin methods are discussed in [30] and upwind mixed FEM are considered in [31,32]; combined finite volume-mixed hybrid finite elements are employed in [33,34].

The primary motivation for the work here is to develop and analyse the appropriate numerical schemes to compute the solution of the Darcy-scale model. Here we assume the flow to be given. Our primary focus is therefore on the convection–diffusion-reaction equation, where the non-linearities are in the reaction term. To avoid dealing with differential inclusions, as the dissolution rate is multi-valued, we use a regularization approach and consider both the semi-discrete and the fully discrete numerical schemes for the resulting (non-linear, but regularized) model. Its solution depends on the regularization parameter. We prove the convergence of the "regularized" solutions to the time-continuous macroscale equations via a limiting procedure, using compactness arguments. Whereas in the case of semi-discrete case, we use translation estimates to improve the convergence needed to deal with the non-linearities, in the fully-discrete case, we use the properties of Lagrange interpolation operator (see [35]) to achieve the required convergence. Of particular relevance to the work presented here are [36], where the convergence of a mixed finite element discretization for the model discussed here is obtained, and [37] where a semi-discrete numerical scheme for pore scale model is considered and the convergence is proved. As in [36], we consider here the upscaled counterpart of the model in [37] and deal with both semi-discrete and fully discrete cases. As a by-product of the convergence proof, we also obtain an alternative proof for existence of solutions for the macroscale equations. The present work is a first step towards an eventual plan to consider both the flow and the reactions coupled together (for example, Richards' equation coupled with precipitation–dissolution reaction models).

The paper is structured as follows. We begin with a brief description of the model in Sect. 2 where we also define the weak solution of the model. We proceed to define the time-discrete formulation in Sect. 3 where the numerical scheme is analyzed and the convergence is proved. Next, in Sect. 4, we consider the fully discrete formulation and treat the convergence issue. The numerical experiments are shown in Sect. 5 followed by the conclusions and discussions in Sect. 6.

2 The model

The presentation of the precipitation–dissolution model considered here is brief; for details we refer to [7–9]. It is relevant to mention that despite the simplification of the model under consideration, the challenging mathematical issues are still present here through the particular choice of the dissolution rate.

Let $\Omega \subset \mathbb{R}^2$ be the domain occupied by the porous medium, and assume Ω be open, connected, bounded and polygonal with Lipschitz boundary Γ. Further, let $T > 0$ be a fixed but arbitrarily chosen time, and define

$$\Omega^T = (0, T] \times \Omega, \quad \text{and} \quad \Gamma^T = (0, T] \times \Gamma.$$

While the reactions take place between the cations and anions, for the model considered here, we study only one mobile species (cation, though the choice is immaterial). This is justified if the boundary and initial data are compatible (see [8], or [9]). Then, denoting by v the concentration of the (immobile) precipitate, and by u the cation

concentration, the model reduces to

$$\begin{cases} \partial_t(u+v) + \nabla \cdot (\mathbf{q}u - \nabla u) = 0, & \text{in} \quad \Omega^T, \\ u = 0, & \text{on} \quad \Gamma^T, \\ u = u_I, & \text{in} \quad \Omega, \ \text{for } t = 0, \end{cases} \tag{2.1}$$

for the ion transport, and

$$\begin{cases} \partial_t v = (r(u) - w), & \text{on} \quad \Omega^T, \\ w \in H(v), & \text{on} \quad \Omega^T, \\ v = v_I, & \text{on} \quad \Omega, \ \text{for } t = 0, \end{cases} \tag{2.2}$$

for the precipitate. The rate of change in the precipitate concentration is the net process of precipitation and dissolution. Here $\mathbf{q}$ stands for the Darcy fluid velocity. We assume that $\mathbf{q}$ is a known, divergence free velocity

$$\nabla \cdot \mathbf{q} = 0 \quad \text{in} \quad \Omega.$$

For the ease of presentation we restrict the analysis to homogeneous Dirichlet boundary conditions. The initial data u_I and v_I are assumed non-negative and essentially bounded. For simplicity we further assume that both $u_I, v_I \in H_0^1(\Omega)$, the space of H^1 functions defined on Ω and having a vanishing trace on Γ.

All quantities and variables in the above are assumed dimensionless. The diffusion is assumed 1, the extension to a positive definite diffusion tensor being straightforward and has no influence on the convergence result here, which is based on compactness arguments. However, if error estimates would have been available (as in the situation when the rates are Lipschitz continuous), the diffusion coefficient would affect directly the constant in the error estimate, but not the convergence order. Similarly, for a positive definite diffusion tensor, one has to use first its Schur decomposition and redefine an (equivalent) norm of the gradient. The singular values influence again the constant in the error estimates. Such issues become important, e.g., in transport dominated regimes, as considered in [14,38]. Of course, from a practical point of view the efficiency of the numerical scheme would suffer, and one would need to consider appropriate (like upwind, see e.g. [31,39,40]) schemes. However, dealing with such aspects is beyond the aim of this contribution. Further, we assume that the Damköhler number is scaled to 1, as well as an eventual factor in the time derivative of v in $(2.1)_1$, appearing in the transition (homogenization) from the pore scale to the core scale. For the precipitation rate r we assume

(A1) $r(\cdot) : \mathbb{R} \to [0, \infty)$ is locally Lipschitz continuous in $\mathbb{R}$.
(A2) There exists a unique $u_* \geq 0$, such that

$$r(u) = \begin{cases} 0 \quad \text{for} \quad u \leq u_*, \\ \text{strictly increasing for} \quad u \geq u_* \quad \text{with} \quad r(\infty) = \infty. \end{cases} \tag{2.3}$$

The dissolution rate has a particular structure. It is assumed constant (1, by scaling) at some $(t, x) \in \Omega^T$ where the precipitate is present, i.e. if $v(t, x) > 0$. In the absence of the precipitate, the overall rate (precipitate minus dissolution) is either zero if the solute present there is insufficient to produce a net precipitation gain, or positive in case the solute exceeds certain threshold value. In the presence of the precipitate, the dissolution strength is constant as it is a surface process. Further, the absence of net precipitation gain under insufficient amount of solutes being present is related to the time-scale of observation. The derivation of the precipitation–dissolution is based on chemical kinetics and the ideas of solubility product for the crystals. For further discussions and derivation of this model, we refer to [7,10]. For the dissolution process, the rate law can be summarized as

$$w \in H(v), \quad \text{where} \quad H(v) = \begin{cases} \{0\}, & \text{if} \quad v < 0, \\ [0, 1], & \text{if} \quad v = 0, \\ \{1\}, & \text{if} \quad v > 0. \end{cases} \tag{2.4}$$

Remark 2.1 Introducing the dissolution rate as above must be completed by a choice of a value $w \in [0, 1]$ at locations where precipitate is absent. As suggested by the existence result for the pore scale model in [11], for a.e. $(t, x) \in \Omega^T$ where $v(t, x) = 0$, the dissolution rate w is chosen to satisfy $w(t, x) = \min\{1, r(u(t, x))\}$ (see also [41] for details).

Remark 2.2 Since the precipitation rate r is monotonically increasing, under the setting above, a unique u^* exists for which $r(u^*) = 1$. Then u^* can be interpreted as an equilibrium value: within an open set $A \subset \Omega^T$ where $u = u^*$, no precipitation or dissolution occurs, and the precipitation rate is balanced by the dissolution rate regardless of the presence or absence of crystals. Then, as follows from [7,11],

$$w = 1 \quad \text{a.e. in} \quad A.$$

Remark 2.3 The upscaled model under discussion, proposed originally in [7] (see also [8–10]), can be obtained by homogenization techniques, starting from its pore scale counterpart in [11].

We emphasize on the particularity of the present model, which is in the description of the dissolution and precipitation processes, involving a multi-valued dissolution rate. Clearly, classical solutions do not exist, except for some particular cases. Therefore we resort to defining appropriate weak solutions. We consider the conformal weak formulation, obtained formally by multiplying the equations (2.1, 2.2) by smooth test functions and using partial integration. We give the exact definition in Sect. 2.2.

2.1 Notations and assumptions

We adopt the following standard notations from the functional analysis. By $(\cdot, \cdot)$ we mean $L^2(\Omega)$ inner product or the duality pairing between H_0^1 and H^{-1}; the $L^2(\Omega^T)$ inner product is denoted by $(\cdot, \cdot)_{\Omega^T}$. Further, $\|\cdot\|$ stands for the norms induced by L^2 inner product, $L^2(0, T; X)$ denotes the usual Bochner spaces for a given Banach

space X. For other norms, we explicitly state it. Furthermore, C denotes the generic constant and the value of which might change from line to line and is independent of unknown variables or the discretization parameters. Let L_r denote the Lipschitz constant of r and $\|\mathbf{q}\|_{L^\infty(\Omega)} \leq M_q$ where M_q is known.

We assume $\Omega \subset \mathbb{R}^2$ to be polygonal and define the following sets

$$\begin{aligned}
\mathcal{U} &:= \{u \in L^2((0,T); H_0^1(\Omega)) : \partial_t u \in L^2((0,T); H^{-1}(\Omega))\},\\
\mathcal{V} &:= \{v \in H^1((0,T); L^2(\Omega))\},\\
\mathcal{W} &:= \{w \in L^\infty(\Omega^T) : 0 \leq w \leq 1\}.
\end{aligned}$$

Since Ω is polygonal, it has a regular decomposition into triangles and the errors due to nonpolygonal domains are avoided. Let $\mathcal{T}_h$ be a regular decomposition of Ω into closed triangles; h stands for the mesh-size. For the fully discrete situation, we will use the discrete subspace $\mathcal{U}_h \subset H_0^1(\Omega)$ defined as

$$\mathcal{U}_h := \{\theta \in C(\bar{\Omega}) \mid \theta \ \in \mathcal{P}_1(T), \quad T \in \mathcal{T}_h, \text{ and } \theta = 0 \text{ on } \partial\Omega\},$$

where $\mathcal{P}_1(T)$ is the space of first order polynomials in two variables, defined on a triangle T. In other words, $\mathcal{U}_h$ denotes the space of piecewise linear functions. Recall that $\mathcal{U}_h \subset H_0^1(\Omega)$ (see [42], p. 64). We also define the following projection:

$$P_h : L^2(\Omega) \mapsto \mathcal{U}_h, (P_h\theta - \theta, \psi_h) = 0, \tag{2.5}$$

for all $\psi_h \in \mathcal{U}_h$. Note that P_h satisfies (see [42], p. 138)

$$\|P_h\theta - \theta\| \leq Ch\|\nabla\theta\|, \tag{2.6}$$

for all $\theta \in H_0^1(\Omega)$, for some $C > 0$ not depending on θ.

Moreover, let $\mathbf{q}_h$ be the discrete approximation of $\mathbf{q}$. We assume $\nabla \cdot \mathbf{q}_h = 0$ with

$$\|\mathbf{q} - \mathbf{q}_h\| \searrow 0$$

as $h \searrow 0$. Further, we assume that $\mathbf{q}_h$ also obeys the maximum principle so that $\|\mathbf{q}_h\|_{L^\infty(\Omega)} \leq M_q$.

2.2 The weak formulation

We start with the definition of a weak solution for (2.1–2.2).

Definition 2.1 A triple $(u, v, w) \in \mathcal{U} \times \mathcal{V} \times \mathcal{W}$ is a weak solution of (2.1) and (2.2) if $(u_{|t=0}, v_{|t=0}) = (u_I, v_I)$, and for all $(\phi, \theta) \in L^2(0, T, H_0^1(\Omega)) \times L^2(0, T; L^2(\Omega))$

$$\begin{aligned}
(\partial_t u + \partial_t v, \phi)_{\Omega^T} + (\nabla u, \nabla\phi)_{\Omega^T} - (\mathbf{q}u, \nabla\phi)_{\Omega^T} &= 0,\\
(\partial_t v, \theta)_{\Omega^T} - (r(u) - H(v), \theta)_{\Omega^T} &= 0,\\
w \in H(v), \text{ a.e. in } \Omega^T,
\end{aligned} \tag{2.7}$$

with the choice $w = \min\{1, r(u)\}$ a.e. in Ω^T where $v = 0$.

The particular choice of the dissolution rate w at points where $v = 0$ is discussed in Remark 2.1. The existence of a weak solution is proved in Theorems 3.10 and 4.8 below. Alternatively, one can obtain the existence as an outcome of the rigorous homogenization procedure, starting from the model at the pore scale. The uniqueness follows by standard contraction arguments. This is summarized in the following

Theorem 2.1 *There exists a unique solution of* (2.7) *in the sense of Definition* 2.1.

Below we prove the convergence of an Euler semi-implicit finite element approximation of the weak solution in Definition 2.1. We start with time-discrete formulation which we refer to as semi-discrete scheme. This provides a good understanding of the mathematical issues encountered in the convergence proofs and prepares the fully-discrete case, where additional issues are encountered due to the projection of the H^1 space onto the finite element space. Quite often, the proofs in the latter case follow the same line of arguments as in the semi-discrete case. In some cases, the results can be directly borrowed; wherever important differences are encountered, these will be commented on below.

3 The semi-discrete scheme

Before defining the time-discretization, let us note the presence of a multi-valued rate in $(2.7)_3$, which impedes obtaining a priori estimates. Therefore we consider a regularized approximation of the original model (and pass later to the limit). We make sure that the estimates are independent of the regularization parameter, which is essential for passing to the limit. With $\delta > 0$, define the regularized Heaviside function

$$H_\delta(v) = \begin{cases} 0, & \text{if } \ v < 0, \\ \frac{v}{\delta}, & \text{if } \ 0 \le v \le \delta, \\ 1, & \text{if } \ v > \delta. \end{cases} \tag{3.1}$$

We use this to introduce the time-discrete scheme. This requires solving at each time t_n a system introduced below as Problem $\mathbf{P}_\delta^n$; the subscript is stressing the dependence on the regularization parameter δ. This gives a sequence of time discrete solutions, which we interpolate in time to obtain a δ-indexed family of functions. Then we use δ and discretization parameter independent a priori estimates to obtain a (weakly) convergent sequence of time interpolants. In the wake of non-linearities involved, we need to improve the convergence, which is obtained by translation estimates in the semi-discrete situation.

Let $N \in \mathbb{N}$ be a given natural number defining a (constant) time step $\tau = \frac{T}{N}$. With $t_n = n\tau$, $n = 1, \dots, N$, we consider a uniform time stepping that is implicit in u and explicit in v. Starting with $u_\delta^0 = u_I$, $v_\delta^0 = v_I$, with $n \in \{1, \dots, N\}$, the approximation (u_δ^n, v_δ^n) of $(u(t_n), v(t_n))$ solves

Problem $\mathbf{P}_\delta^n$: Given $(u_\delta^{n-1}, v_\delta^{n-1}) \in H_0^1(\Omega) \times L^2(\Omega)$, find $(u_\delta^n, v_\delta^n) \in H_0^1(\Omega) \times L^2(\Omega)$ such that

$$\left(\frac{u_\delta^n - u_\delta^{n-1}}{\tau}, \phi\right) + (\nabla u_\delta^n, \nabla\phi) - (\mathbf{q}u_\delta^n, \nabla\phi) + \left(\frac{v_\delta^n - v_\delta^{n-1}}{\tau}, \phi\right) = 0$$
$$\left(\frac{v_\delta^n - v_\delta^{n-1}}{\tau}, \theta\right) = \left(r(u_\delta^n) - H_\delta(v_\delta^{n-1}), \theta\right), \tag{3.2}$$

for all $\phi \in H_0^1(\Omega), \theta \in L^2(\Omega)$. For completeness, we define

$$w_\delta^n := H_\delta(v_\delta^n).$$

For stability reasons, we choose $\delta = O(\tau^{\frac{1}{2}})$. In particular, this choice provides the result in Lemma 3.8; details about this choice are also provided in [37]. Nevertheless, numerical computations reported in [19] suggest that practically it is sufficient to choose $\delta = C\tau$ with $C > 1$.

Problem $\mathbf{P}_\delta^n$ is a system of elliptic equations for u_δ^n, v_δ^n given $u_\delta^{n-1} \in H_0^1(\Omega), v_\delta^{n-1} \in L^2(\Omega)$. Note that the first equation is decoupled from the second equation since it can be written in the form

$$\left(\frac{u_\delta^n - u_\delta^{n-1}}{\tau}, \phi\right) + (\nabla u_\delta^n, \nabla\phi) - (\mathbf{q}u_\delta^n, \nabla\phi) + \left(r(u_\delta^n) - H_\delta(v_\delta^{n-1}), \phi\right) = 0.$$

The reaction term r being Lipschitz and increasing, standard monotonicity arguments can be used to show the existence and uniqueness of u_δ^n given u_δ^{n-1} [43]. After u_δ^n is computed, v_δ^n is obtained explicitly from $(3.2)_2$. We summarize this into:

Lemma 3.1 *Problem $\mathbf{P}_\delta^n$ has a unique solution pair (u_δ^n, v_δ^n).*

For the continuous formulation (2.7), the solutions u and v are expected to be positive and essentially bounded. Here we prove this property for the time-discrete formulation. With $M_u := \max\{\|u_I\|_{L^\infty}, u^*\}, M_v := \|v_I\|_{L^\infty}$, we note that $r(M_u) \geq 1$. We start with the positivity of the solution pair (u_δ^n, v_δ^n).

Lemma 3.2 *If u_δ^{n-1} and v_δ^{n-1} are non-negative, then the same holds for u_δ^n and v_δ^n.*

Proof First we consider v_δ^n. With $[\cdot]_-$ denoting the non-positive part, we take $\theta = [v_\delta^{n-1}]_-$ in $(3.2)_2$ to get

$$\|[v_\delta^n]_-\|^2 = \left(v_\delta^{n-1}, [v_\delta^n]_-\right) + \tau\left(r(u_\delta^n) - H_\delta(v_\delta^{n-1}), [v_\delta^n]_-\right).$$

By assumption, $v_\delta^{n-1} \geq 0$, $\delta = O(\tau^{\frac{1}{2}})$ and $r(u_\delta^n) \geq 0$, yielding

$$v_\delta^{n-1} - \tau H_\delta(v_\delta^{n-1}) \geq v_\delta^{n-1}(1 - \tau/\delta) \geq 0.$$

Therefore $\|[v_\delta^n]_-\|^2 \le 0$ implying $v_\delta^n \ge 0$.

Next we prove that u_δ^n is non-negative. For $\phi = [u_\delta^n]_-$ in $(3.2)_1$

$$\|[u_\delta^n]_-\|^2 + \tau\|\nabla[u_\delta^n]_-\|^2 - \tau\left(\mathbf{q}u_\delta^n, \nabla[u_\delta^n]_-\right) + \left(v_\delta^n - v_\delta^{n-1}, [u_\delta^n]_-\right) \le \left(u_\delta^{n-1}, [u_\delta^n]_-\right).$$

The first two terms are non-negative, whereas the third term vanishes:

$$(\mathbf{q}u_\delta^n, \nabla[u_\delta^n]_-) = \frac{1}{2}\left(\mathbf{q}, \nabla[u_\delta^n]_-^2\right) = \frac{1}{2}\left(\nu\cdot\mathbf{q}, [u_\delta^n]_-^2\right)_\Gamma - \frac{1}{2}\left(\nabla\cdot\mathbf{q}, [u_\delta^n]_-^2\right) = 0,$$

by the boundary conditions for u_δ^n on Γ and since $\nabla\cdot\mathbf{q} = 0$ in Ω. Further, by $(3.2)_2$

$$\left(v_\delta^n - v_\delta^{n-1}, [u_\delta^n]_-\right) = \tau\left(r(u_\delta^n) - H_\delta(v_\delta^{n-1}), [u_\delta^n]_-\right) = -\tau\left(H_\delta(v_\delta^{n-1}), [u_\delta^n]_-\right) \ge 0,$$

where we have used Assumption (A2), ensuring that $r(u)\,u = 0$ for all negative u, and the positivity of H_δ. Since $u_\delta^{n-1} \ge 0$, we obtain $u_\delta^n \ge 0$. □

The next lemma provides an upper bound (uniformly w.r.t. n and δ) for the concentration u_δ^n; its proof is based on a simple induction argument.

Lemma 3.3 *If $u_\delta^{n-1} \le M_u$ then $u_\delta^n \le M_u$.*

Proof Test $(3.2)_1$ with $\phi = [u_\delta^n - M_u]_+$ (the non-negative part of $u_\delta^n - M_u$) to obtain

$$\begin{aligned}\|[u_\delta^n - M_u]_+\|^2 + \tau\|\nabla[u_\delta^n - M_u]_+\|^2 - \tau(\mathbf{q}u_\delta^n, \nabla[u_\delta^n - M_u]_+)\\ +(v_\delta^n - v_\delta^{n-1}, [u_\delta^n - M_u]_+) \le (u_\delta^{n-1} - M_u, [u_\delta^n - M_u]_+).\end{aligned} \tag{3.3}$$

As before, the third term vanishes. Further observe that $r(u_\delta^n) - H_\delta(v_\delta^{n-1}) \ge 0$ wherever $u_\delta^n \ge M_u$, implying

$$(v_\delta^n - v_\delta^{n-1}, [u_\delta^n - M_u]_+) = (r(u_\delta^n) - H_\delta(v_\delta^{n-1}), [u_\delta^n - M_u]_+) \ge 0.$$

Finally, since $u_\delta^{n-1} - M_u \le 0$ one gets $(u_\delta^{n-1} - M_u, [u_\delta^n - M_u]_+) \le 0$, which concludes the proof. □

As v satisfies an ordinary differential equation having no equilibria, no uniform (time independent) upper bound can be expected for the precipitate concentration. In this spirit, the time discrete v_δ^n still satisfies upper bounds, but increasing with $n\tau$:

Lemma 3.4 *Let $C = \frac{L_r M_u}{M_v}$ and assume that $v_\delta^{n-1} \le M_v e^{C(n-1)\tau}$, then $v_\delta^n \le M_v e^{Cn\tau}$.*

Proof We use $\theta := [v_\delta^n - M_v e^{Cn\tau}]_+$ in $(3.2)_2$ to obtain

$$\begin{aligned}\|[v_\delta^n - M_v e^{Cn\tau}]_+\|^2 = &\left(v_\delta^{n-1} - M_v e^{C(n-1)\tau}, [v_\delta^n - M_v e^{Cn\tau}]_+\right)\\ &+ M_v\left(e^{C(n-1)\tau} - e^{Cn\tau}, [v_\delta^n - M_v e^{Cn\tau}]_+\right)\\ &\times\tau\left(r(u_\delta^n) - H_\delta(v_\delta^{n-1}), [v_\delta^n - M_v e^{Cn\tau}]_+\right).\end{aligned} \tag{3.4}$$

Since $r(u_\delta^n)$ is Lipschitz and $H_\delta(\cdot)$ is positive, one has

$$\tau\left(r(u_\delta^n) - H_\delta(v_\delta^{n-1}), [v_\delta^n - M_v e^{Cn\tau}]_+\right) \le \tau(CM_v, [v_\delta^n - M_v e^{Cn\tau}]_+),$$

and

$$M_v\left(e^{C(n-1)\tau} - e^{Cn\tau}, [v_\delta^n - M_v e^{Cn\tau}]_+\right) \le M_v\left(1 - e^{C\tau}, [v_\delta^n - M_v e^{Cn\tau}]_+\right).$$

Here, we have used $e^{C(n-1)\tau} \ge 1$. Next, since $1 + x \le e^x$ for any $x \ge 0$,

$$\begin{aligned}&\tau\left(CM_v, [v_\delta^n - M_v e^{Cn\tau}]_+\right) + M_v\left(1 - e^{C\tau}, [v_\delta^n - M_v e^{Cn\tau}]_+\right)\\ &\le M_v\left(C\tau + 1 - e^{C\tau}, [v_\delta^n - M_v e^{Cn\tau}]_+\right) \le 0.\end{aligned}$$

Recalling the assumption on v_δ^{n-1}, we have $\left(v_\delta^{n-1} - M_v e^{C(n-1)\tau}, [v_\delta^n - M_v e^{Cn\tau}]_+\right) \le 0$. Using this in (3.4), we conclude that

$$\|[v_\delta^n - M_v e^{Cn\tau}]_+\|^2 \le 0,$$

which proves the conclusion. □

Remark 3.1 As $n\tau = t_n \le T$, the estimates shown above are independent of δ and τ.

3.1 Stability estimates

With the pointwise bounds for the Problem $\mathbf{P}_\delta^n$ already established, we proceed to obtain stability estimates. These estimates will be used later for compactness arguments and are similar to those for parabolic equations, but here restricted to discrete time steps. We have:

Lemma 3.5 *A constant C independent of τ and δ exists s.t. the following estimates hold*

$$\max_{n=1,\dots,N} \|v_\delta^n\| \le \|v_I\| + Cr(M_u), \tag{3.5}$$

$$\max_{n=1,\dots,N} \|v_\delta^n - v_\delta^{n-1}\| + \sum_{n=1}^{N} \|u_\delta^n - u_\delta^{n-1}\|^2 \le C\tau, \tag{3.6}$$

$$\sum_{n=1}^{N} \|\nabla(u_\delta^n - u_\delta^{n-1})\|^2 + \tau \sum_{n=1}^{N} \|\nabla u_\delta^n\|^2 \le C. \tag{3.7}$$

Proof To prove (3.5) we choose the test function $\phi = v_\delta^n$ in $(3.2)_2$ to obtain

$$(v_\delta^n - v_\delta^{n-1}, v_\delta^n) = \tau\left(r(u_\delta^n) - H_\delta(v_\delta^{n-1}), v_\delta^n\right).$$

Using Cauchy–Schwarz inequality, monotonicity of r and H_δ, $v_\delta^n \geq 0$, this gives

$$\|v_\delta^n\|^2 \leq \|v_\delta^n\| \left(\|v_\delta^{n-1}\| + C\tau r(M_u) \right).$$

Dividing in the above by $\|v_\delta^n\|$ (the case $\|v_\delta^n\| = 0$ being trivial) and summing the resulting over n gives (3.5).

To prove the first part of (3.6), we take $\theta = v_\delta^n - v_\delta^{n-1}$ into $(3.2)_2$ and obtain

$$\|v_\delta^n - v_\delta^{n-1}\|^2 = \tau \left(r(u_\delta^n) - H_\delta(v_\delta^n), v_\delta^n - v_\delta^{n-1} \right) \leq \tau^2 \frac{1}{2} (r(M_u))^2 + \frac{1}{2}\tau^2 + \frac{1}{2}\|v_\delta^n - v_\delta^{n-1}\|^2,$$

providing immediately the first part of (3.6).

For second part of (3.7) we choose $\phi = u_\delta^n$ in $(3.2)_1$ to obtain

$$(u_\delta^n - u_\delta^{n-1}, u_\delta^n) + \tau \|\nabla u_\delta^n\|^2 - \tau(\mathbf{q} u_\delta^n, \nabla u_\delta^n) + (v_\delta^n - v_\delta^{n-1}, u_\delta^n) = 0,$$

which gives

$$\frac{1}{2} \left(\|u_\delta^n\|^2 - \|u_\delta^{n-1}\|^2 + \|u_\delta^n - u_\delta^{n-1}\|^2 \right) + \tau \|\nabla u_\delta^n\|^2 \leq \|v_\delta^n - v_\delta^{n-1}\| \|u_\delta^n\| \leq C\tau.$$

A summation over $n = 1, \ldots, k$ ($k \leq N$ being arbitrary) leads to

$$\frac{1}{2}\|u_\delta^k\|^2 + \frac{1}{2} \sum_{n=1}^{k} \|u_\delta^n - u_\delta^{n-1}\|^2 + \tau \sum_{n=1}^{k} \|\nabla u_\delta^n\|^2 \leq \frac{1}{2}\|u_I\|^2 + C \leq C.$$

This gives straightforwardly the desired bound.

For the remaining estimates we take $\phi = u_\delta^n - u_\delta^{n-1}$ in $(3.2)_1$ and obtain

$$\begin{aligned} &\|u_\delta^n - u_\delta^{n-1}\|^2 + \tau \left(\nabla u_\delta^n, \nabla (u_\delta^n - u_\delta^{n-1}) \right) + \tau \left(\mathbf{q} u_\delta^n, \nabla (u_\delta^n - u_\delta^{n-1}) \right) \\ &\quad + (v_\delta^n - v_\delta^{n-1}, u_\delta^n - u_\delta^{n-1}) = 0. \end{aligned}$$

The terms on the left hand side can be estimated by

$$\begin{aligned} \tau(\nabla u_\delta^n, \nabla (u_\delta^n - u_\delta^{n-1})) &= \tau \frac{1}{2} \left(\|\nabla u_\delta^n\|^2 - \|\nabla u_\delta^{n-1}\|^2 + \|\nabla (u_\delta^n - u_\delta^{n-1})\|^2 \right), \\ \tau \left| (\nabla \cdot (\mathbf{q} u_\delta^n), (u_\delta^n - u_\delta^{n-1})) \right| &\leq \frac{\tau^2 M_q^2 \|\nabla u_\delta^n\|^2}{2} + \frac{1}{2}\|u_\delta^n - u_\delta^{n-1}\|^2, \\ \left| (v_\delta^n - v_\delta^{n-1}, u_\delta^n - u_\delta^{n-1}) \right| &\leq \left(\|v_\delta^n - v_\delta^{n-1}\|^2 + \frac{1}{4}\|u_\delta^n - u_\delta^{n-1}\|^2 \right) \\ &\leq C\tau^2 + \frac{1}{4}\|u_\delta^n - u_\delta^{n-1}\|^2, \end{aligned}$$

where for the last line we have used the inequality for v_δ^n in (3.6). As above, summing over $n = 1, \ldots, k$ (with $k \leq N$ arbitrary) leads to

$$\frac{1}{4}\sum_{n=1}^{k}\|u_\delta^n - u_\delta^{n-1}\|^2 + \tau\|\nabla u_\delta^k\|^2 + \tau\sum_{n=1}^{k}\|\nabla(u_\delta^n - u_\delta^{n-1})\|^2$$
$$\leq C\tau + CM_q^2\tau + \tau\|\nabla u_I\|^2 \leq C\tau,$$

and the proof is concluded. □

3.2 The convergence

Here we consider the sequence of time discrete $(u_\delta^n, v_\delta^n, w_\delta^n)$ solving problem $\mathbf{P}_\delta^n$, and construct a time continuous approximation by taking linear interpolation. For each N and $\tau = T/N$ we define,

$$U^\tau(t) := u_\delta^n\frac{(t-t_{n-1})}{\tau} + u_\delta^{n-1}\frac{(t_n - t)}{\tau}, \tag{3.8}$$
$$V^\tau(t) := v_\delta^n\frac{(t-t_{n-1})}{\tau} + v_\delta^{n-1}\frac{(t_n - t)}{\tau}, \tag{3.9}$$
$$W^\tau(t) := H_\delta(V^\tau(t)). \tag{3.10}$$

Note that the index δ is suppressed (for the ease of writing) as we assume here that the regularization parameter and the time step are related (by $\delta = O(\tau^{\frac{1}{2}})$). We have introduced in fact a sequence of triples $\{(U^\tau, V^\tau, W^\tau)\}_{N\in\mathbb{N}}$, for which we use compactness arguments and identify limit points, which are weak solutions as introduced in Definition 2.1. To this aim we use the estimates in (3.5–3.7) and prove

Lemma 3.6 *A constant $C > 0$ independent of τ and δ exists s.t. the following estimates hold:*

$$0 \leq U^\tau \leq M_u, 0 \leq V^\tau \leq M_v e^{CT}, 0 \leq W^\tau \leq 1 \tag{3.11}$$
$$\|U^\tau\|^2 + \|V^\tau\|^2 \leq C, \tag{3.12}$$
$$\|\partial_t U^\tau\|^2 + \|\nabla U^\tau\|^2 + \|\partial_t V^\tau\|^2 \leq C. \tag{3.13}$$

Proof Clearly, (3.11, 3.12) follow directly from the L^∞ estimates for u_δ^n, v_δ^n. We therefore start with the gradient estimates. In view of (3.8),

$$\|\nabla U^\tau\|^2 \leq 2\|\nabla u_\delta^{n-1}\|^2 + 2\frac{(t-t_{n-1})^2}{\tau^2}\|\nabla(u_\delta^n - u_\delta^{n-1})\|^2,$$

which can be integrated over t to obtain

$$\int_0^T \|\nabla U^\tau\|^2 dt \leq \sum_{n=1}^{N} 2\int_{t_{n-1}}^{t_n}\|\nabla u_\delta^{n-1}\|^2 dt + 2\sum_{n=1}^{N}\int_{t_{n-1}}^{t_n}\frac{(t-t_{n-1})^2}{\tau^2}\|\nabla(u_\delta^n - u_\delta^{n-1})\|^2 dt,$$
$$\leq \sum_{n=1}^{N} 2\tau\|\nabla u_\delta^{n-1}\|^2 + \sum_{n=1}^{N}\frac{2\tau}{3}\|\nabla(u_\delta^n - u_\delta^{n-1})\|^2.$$

The stability estimates in (3.7) provide the gradient estimates in (3.13).

To estimate $\|\partial_t V^\tau\|_{L^2(\Omega^T)}$ we note that for whenever $t \in (t_{n-1}, t_n]$ one has $\partial_t V^\tau = \frac{v_\delta^n - v_\delta^{n-1}}{\tau}$, implying

$$\int_0^T \|\partial_t V^\tau\|^2 dt = \sum_{n=1}^N \int_{t_{n-1}}^{t_n} \|\frac{v_\delta^n - v_\delta^{n-1}}{\tau}\|^2 dt \le \sum_{n=1}^N \tau \|\frac{v_\delta^n - v_\delta^{n-1}}{\tau}\|^2 \le CN\tau \le CT \le C,$$

where we have used the estimate (3.6).

Finally, the estimates on $\partial_t U^\tau$ are similar. Observing that $\partial_t U^\tau = \frac{u_\delta^n - u_\delta^{n-1}}{\tau}$ whenever $t \in (t_{n-1}, t_n]$, integrating over t yields

$$\int_0^T \|\partial_t U^\tau\|^2 dt = \sum_{n=1}^N \int_{t_{n-1}}^{t_n} \|\frac{u_\delta^n - u_\delta^{n-1}}{\tau}\|^2 dt \le \sum_{n=1}^N \tau \|\frac{u_\delta^n - u_\delta^{n-1}}{\tau}\|^2 \le CN\tau \le CT \le C,$$

where we have used the estimate (3.6). In this way the lemma is proved. □

The estimates in Lemma 3.6 are uniform in τ and δ. Furthermore, we have $(U^\tau, V^\tau, W^\tau) \in \mathcal{U} \times \mathcal{V} \times \mathcal{W}$. Clearly, $\tau \searrow 0$ with $\delta = O(\tau^{\frac{1}{2}})$ implies that both $\delta, \frac{\tau}{\delta} \searrow 0$. By the Eberlein–Smulian and Banach–Alaoglu theorems one has the following convergence result.

Lemma 3.7 *There exists a triple $(u, v, w) \in \mathcal{U} \times \mathcal{V} \times \mathcal{W}$ such that along a sequence $\tau \searrow 0$ one has*

1. $U^\tau \rightharpoonup u$ *weakly in* $L^2((0,T); H_0^1(\Omega))$,
2. $\partial_t U^\tau \rightharpoonup \partial_t u$ *weakly in* $L^2((0,T); H^{-1}(\Omega))$,
3. $V^\tau \rightharpoonup v$ *weakly in* $L^2((0,T); L^2(\Omega))$,
4. $\partial_t V^\tau \rightharpoonup \partial_t v$ *weakly in* $L^2((0,T); L^2(\Omega))$,
5. $W^\tau \rightharpoonup w$ *weakly-star in* $L^\infty(\Omega)$.

Having defined the limit triple (u, v, w), it remains to prove that it is a weak solution in the sense of Definition 2.1. We start by noting that the first two convergence results in Lemma 3.7 give the strong convergence (see [44])

$$U^\tau \to u \quad \text{strongly in} \quad L^2((0,T); L^2(\Omega)). \tag{3.14}$$

Further, this lemma only provides a weak convergence for V^τ. In the wake of nonlinearities, an improved (strong) convergence for V^τ is required here as well. This is obtained by showing that, assuming the H^1 regularity of the initial datum, V^τ and v have the same spatial regularity. The proof relies on translation estimates. In this sense, let $t \in (t_{n-1}, t_n] (0 < n \le N)$ be a fixed time and define $\triangle_\xi$ as the translation operator

$$\triangle_\xi f(y,t) = f(y,t) - f(y+\xi, t). \tag{3.15}$$

To prove the translation estimate we fix N (and hence τ and δ). We have:

Lemma 3.8 *If $v_I \in H^1(\Omega)$ then the following estimate holds*

$$\max_{k=1,\dots,N} \left\| \triangle_\xi v_\delta^k \right\|^2 + \sum_{n=1}^{N} \left\| \triangle_\xi (v_\delta^n - v_\delta^{n-1}) \right\|^2 \le C \left\| \triangle_\xi v_I \right\|^2 + C\tau \sum_{n=1}^{N} \left\| \triangle_\xi u_\delta^n \right\|^2 . \tag{3.16}$$

Proof For $\theta = \triangle_\xi v_\delta^n$ in $(3.2)_2$, we get

$$\left(\triangle_\xi v_\delta^n - \triangle_\xi v_\delta^{n-1}, \triangle_\xi v_\delta^n \right) = \tau \left(\triangle_\xi r(u_\delta^n), \triangle_\xi v_\delta^n \right) - \tau \left(\triangle_\xi H_\delta(v_\delta^{n-1}), \triangle_\xi v_\delta^n \right). \tag{3.17}$$

The last term in the above rewrites

$$\left(\triangle_\xi H_\delta(v_\delta^{n-1}), \triangle_\xi v_\delta^n \right) = \left(\triangle_\xi H_\delta(v_\delta^{n-1}), \triangle_\xi v_\delta^{n-1} \right) + \left(\triangle_\xi H_\delta(v_\delta^{n-1}), \triangle_\xi (v_\delta^n - v_\delta^{n-1}) \right).$$

The first term on the right is positive due to the monotonicity of H_δ. For the left hand side, we use the identity

$$\left(\triangle_\xi v_\delta^n - \triangle_\xi v_\delta^{n-1}, \triangle_\xi v_\delta^n \right) = \frac{1}{2} \left(\left\| \triangle_\xi v_\delta^n \right\|^2 - \left\| \triangle_\xi v_\delta^{n-1} \right\|^2 + \left\| \triangle_\xi (v_\delta^n - v_\delta^{n-1}) \right\|^2 \right).$$

By the Cauchy–Schwarz inequality, (3.17) becomes

$$\begin{aligned} &\frac{1}{2} \left(\left\| \triangle_\xi v_\delta^n \right\|^2 - \left\| \triangle_\xi v_\delta^{n-1} \right\|^2 + \left\| \triangle_\xi (v_\delta^n - v_\delta^{n-1}) \right\|^2 \right) \\ &\quad \le \frac{\tau}{2} \left\| \triangle_\xi r(u_\delta^n) \right\|^2 + \frac{\tau}{2} \left\| \triangle_\xi v_\delta^n \right\|^2 + \tau^2 \left\| \triangle_\xi H_\delta(v_\delta^{n-1}) \right\|^2 + \frac{1}{4} \left\| \triangle_\xi (v_\delta^n - v_\delta^{n-1}) \right\|^2 . \end{aligned}$$

Since r and H_δ are Lipschitz continuous this leads to

$$\begin{aligned} &\left\| \triangle_\xi v_\delta^n \right\|^2 - \left\| \triangle_\xi v_\delta^{n-1} \right\|^2 + \frac{1}{2} \left\| \triangle_\xi (v_\delta^n - v_\delta^{n-1}) \right\|^2 \\ &\quad \le L_{r^2} \tau \left\| \triangle_\xi u_\delta^n \right\|^2 + \tau \left\| \triangle_\xi v_\delta^n \right\|^2 + \frac{2\tau^2}{\delta^2} \| \triangle_\xi v_\delta^{n-1} \|^2 . \end{aligned}$$

Summing the above over $n = 1, \dots, k$ (with $k \le N$ arbitrary) gives

$$\begin{aligned} &\left\| \triangle_\xi v_\delta^k \right\|^2 + \frac{1}{2} \sum_{n=1}^{k} \left\| \triangle_\xi (v_\delta^n - v_\delta^{n-1}) \right\|^2 \\ &\quad \le \left\| \triangle_\xi v_I \right\|^2 + L_{r^2} \tau \sum_{n=1}^{k} \left\| \triangle_\xi u_\delta^n \right\|^2 + \tau \sum_{n=1}^{k} \left\| \triangle_\xi v_\delta^n \right\|^2 + \sum_{n=1}^{k} \frac{2\tau^2}{\delta^2} \| \triangle_\xi v_\delta^{n-1} \|^2 . \end{aligned} \tag{3.18}$$

With $\delta = O(\sqrt{\tau})$, the conclusion is a direct consequence of the discrete Gronwall inequality. □

The translation estimates in Lemma 3.8 above provide the strong convergence of V^τ:

Lemma 3.9 *Along a sequence $\tau \searrow 0$ one has*

$$V^\tau \to v \quad \textit{strongly in} \quad L^2(0,T;L^2(\Omega)). \tag{3.19}$$

Proof The proof is based on the Riesz–Frechet–Kolmgorov compactness criterion (see e.g. Theorem 4.26 in [45]) and uses translation estimates in space and time. First, let Ω' denote an arbitrary compact subset of Ω and $\xi \in (0, dist(\Gamma, \Omega'))$. The strong convergence is tantamount to proving that

$$\mathcal{I} := \int\limits_{\Omega' T} |V^\tau(t+h_t, x+\xi) - V^\tau(t,x)|^2 dxdt \searrow 0 \quad \text{as} \quad |(h_t,\xi)'| \searrow 0.$$

Since $\partial_t V^\tau$ is bounded uniformly in $L^2(0,T;L^2(\Omega))$, the estimates for the translation with respect to time are straightforward. We therefore consider the translation with respect to space.

Using the definition of V^τ, one has

$$\triangle_\xi V^\tau = \frac{t_n - t}{\tau} \triangle_\xi v_\delta^{n-1} + \frac{t - t_{n-1}}{\tau} \triangle_\xi v_\delta^n.$$

Squaring and integrating the left hand side over $\Omega' \times (0,T)$ gets

$$\int\limits_0^T \int\limits_{\Omega'} |\triangle_\xi V^\tau|^2 \le C\tau \sum_{n=1}^N \|\triangle_\xi v_\delta^n\|^2.$$

As in the proof of Lemma 3.8, the right hand side is estimated as

$$\int\limits_0^T \int\limits_{\Omega'} \left|\triangle_\xi V^\tau(t,x)\right|^2 dxdt \le CT\tau \sum_{n=1}^N \left\|\triangle_\xi u_\delta^n\right\|^2 + CT \left\|\triangle_\xi v_I\right\|^2.$$

Before proceeding with the estimates we note that one can use the sequence of time discrete approximations u_δ^n $(n = 1, \ldots, N)$ to define the piecewise constant interpolation $\bar{U}^\tau : [0,T] \to L^2(0,T;H_0^1(\Omega))$, $\bar{U}^\tau(t) = u_\delta^n$ if $t \in [t_{n-1}, t_n)$. With this we exploit a general result (for example, see [46]) which connects the convergence of piecewise linear interpolations (here U^τ, which converges strongly to u in $L^2(0,T;L^2(\Omega))$) with that of the piecewise constant interpolations. We therefore obtain that $\bar{U}^\tau$ converges strongly to u in $L^2(0,T;L^2(\Omega))$ as well, and therefore the space translations are controlled (see [45], Chapter 4), namely

$$\tau \sum_{n=1}^N \left\|\triangle_\xi \bar{U}^\tau\right\|^2 \searrow 0 \quad \text{as} \quad |\xi| \searrow 0.$$

Furthermore, since the initial conditions are in $H^1(\Omega)$, $\left\|\triangle_\xi v_I\right\|^2 \searrow 0$ as $|\xi| \searrow 0$. With this, $\mathcal{I} \searrow 0$ as $|\xi| \searrow 0$ which proves the strong convergence of V^τ. □

Having established the strong convergence for V^τ, we can now show that the limit triple (u, v, w) in Lemma 3.7 is a weak solution of (2.1, 2.2):

Theorem 3.10 *The limit triple (u, v, w) is a weak solution in the sense of Definition 2.1.*

Proof By the weak convergence, the estimates in Lemma 3.6 carry over for the limit triple (u, v, w). Moreover,

$$\int_0^T (\partial_t U^\tau, \phi)dt + \int_0^T (\nabla U^\tau, \nabla\phi)dt + \int_0^T (\mathbf{q}\cdot\nabla U^\tau, \phi)dt + \int_0^T (\partial_t V^\tau, \phi)dt$$
$$= \sum_{n=1}^N \int_{t_{n-1}}^{t_n} ((\nabla U^\tau - \nabla u_\delta^n), \nabla\phi)dt + \sum_{n=1}^N \int_{t_{n-1}}^{t_n} (\mathbf{q}\cdot(\nabla U^\tau - \nabla u_\delta^n), \phi)dt,$$

for all $\phi \in L^2(0, T; H_0^1(\Omega))$. By Lemma 3.7, the left hand side converges to the desired limit. We are thus required to show that the terms on the right, denoted by $\mathcal{I}_1$ and $\mathcal{I}_2$, are vanishing with $\tau \searrow 0$. This is a direct consequence of (3.7), as

$$|\mathcal{I}_1| \le \tau^{\frac{1}{2}} \left(C \sum_{n=1}^N \|\nabla u_\delta^n - \nabla u_\delta^{n-1}\|^2 \right)^{\frac{1}{2}} \left(\int_0^T \|\nabla\phi\|^2 dt \right)^{\frac{1}{2}}, \quad \text{and}$$

$$|\mathcal{I}_2| \le \tau^{\frac{1}{2}} \left(\sum_{n=1}^N \tau M_q \|\nabla(u_\delta^n - u_\delta^{n-1})\|^2 \right)^{\frac{1}{2}} \left(\int_0^T \|\phi\|^2 dt \right)^{\frac{1}{2}}.$$

For the limit equation for V^τ, we use $(3.2)_2$ to obtain

$$\int_0^T (\partial_t V^\tau, \theta)dt = \int_0^T (r(U^\tau) - W^\tau)dt + \sum_{n=1}^N \int_{t_{n-1}}^{t_n} (r(u_\delta^n) - r(U^\tau), \theta)dt$$
$$+ \sum_{n=1}^N \int_{t_{n-1}}^{t_n} (W^\tau - H_\delta(v_\delta^{n-1}), \theta)dt.$$

The desired limit equations is retrieved once it is proved that the last two integrals on the right hand side, denoted by $\mathcal{I}_3$ and $\mathcal{I}_4$, vanish. This is obtained as above, but using now (3.6). We have

$$|\mathcal{I}_3| \le \tau^{\frac{1}{2}} L_r \left(\sum_{n=1}^{N} \|u_\delta^n - u_\delta^{n-1}\|^2 \right)^{\frac{1}{2}} \left(\int_0^T \|\theta\|^2 dt \right)^{\frac{1}{2}},$$

approaching 0 as $\tau \searrow 0$. For $\mathcal{I}_4$, use the definition of W^τ and Lipschitz continuity of H_δ in order to obtain

$$|\mathcal{I}_4| \le \sum_{n=1}^{N} \int_{t_{n-1}}^{t_n} \frac{1}{\delta} \|v_\delta^n - v_\delta^{n-1}\| \|\theta\| dt \le C \frac{\tau}{\delta} \left(\int_0^T \|\theta\|^2 dt \right)^{\frac{1}{2}},$$

by using (3.6) and the Cauchy–Schwarz inequality. Since δ is chosen s.t. $\tau/\delta \searrow 0$ we get $\mathcal{I}_4 \searrow 0$.

Finally we need to prove $w \in H(v)$. The strong L^2 convergence of V^τ also provides the a.e. convergence $V^\tau \to v$. Further, as $\tau \searrow 0$, the weak* convergence of W^τ gives

$$(W^\tau, \theta) \to (w, \theta), \quad \text{and} \quad 0 \le w \le 1 \text{ (a.e.)}.$$

To prove that $w \in H(v)$ indeed we take a pair $(t, x) \in \Omega$ and distinguish two cases: either $v(t, x) > 0$, or $v(t, x) = 0$. In the former we recall that $W^\tau = H_\delta(V^\tau)$ (by definition) and that $\tau \searrow 0$ also implies $\delta \searrow 0$. Then the pointwise (a.e.) convergence of V^τ implies that for all $\tau < \tau_0$ (with sufficiently small τ_0) we have $V^\tau(t, x) > v(t, x)/2 > \delta > 0$, yielding $W^\tau = H_\delta(V^\tau(t, x)) = 1$ and hence $w = 1$. In subsets of Ω^T where $v = 0$, since $\partial_t v \in L^2(\Omega)$ one has $\partial_t v = 0$ a.e., leading to $w = r(u)$ with $0 \le w \le 1$, which proves the final step. □

Remark 3.2 As mentioned in the introduction, the convergence proof for the semi-discrete approximation is also an existence proof for a weak solution. The uniqueness can be obtained by contraction arguments, see e.g. Theorem 4.7 in [11].

4 The fully discrete scheme

Here we extend the convergence result to the fully discrete scheme, obtained by the finite element discretization of the semi-discrete problems in Sect. 3. The convergence proof follows the same ideas, and therefore we restrict the details to a minimum. To simplify notation, henceforth, we suppress the subscript δ.

The fully discrete approximation of the weak solution of (2.1, 2.2) builds on the semi-implicit (implicit in u and explicit in v) discretization introduced in (3.2).

Starting with $u_h^0 = P_h u_I$, $v_h^0 = P_h v_I$ (the projection of the initial data onto the finite element space $\mathcal{U}_h$ introduced in Sect. 2.1), with $n \in \{1, \ldots, N\}$, the approximation (u_h^n, v_h^n) of $(u(t_n), v(t_n))$ at $\mathcal{T}_h$ solves

Problem $\mathbf{P}_h^n$: Given $u_h^{n-1}, v_h^{n-1} \in \mathcal{U}_h$, find u_h^n and $v_h^n \in \mathcal{U}_h$ such that for all $\phi_h, \theta_h \in \mathcal{U}_h$,

$$(u_h^n - u_h^{n-1}, \phi_h) + \tau(\nabla u_h^n, \nabla \phi_h) - (\mathbf{q}_h u_h^n, \nabla \phi_h) + (v_h^n - v_h^{n-1}, \phi_h) = 0,$$
$$(v_h^n - v_h^{n-1}, \theta_h) - \tau(r(u_h^n), \theta_h) + \tau(H_\delta(v_h^{n-1}), \theta_h) = 0. \quad (4.1)$$

To complete the solution we also define $w_h^n := H_\delta(v_h^n) \in L^\infty(\Omega)$.

4.1 Existence and uniqueness

The problems introduced above form a sequence of nonlinear (algebraic) systems. As in the semi-discrete case, for stability reasons we choose $\delta = O(\tau^{\frac{1}{2}})$. The first task here is to prove the existence and uniqueness of a solution for problem $\mathbf{P}_h^n$. Since $\mathbf{P}_h^n$ is defined on a finite dimensional space, the existence can be obtained e.g. by a fixed point argument in [47] (Lemma 1.4, p. 140). Here we present an alternative fixed point argument based on linearization techniques (see [48]). In this way, next to the proof for the existence and uniqueness of a solution, we also define a convergent linear iteration scheme for solving the fully discrete nonlinear systems. This method is employed to perform the numerical computations in Sect. 5, which justifies our choice here.

Below we assume that u_h^{n-1} and v_h^{n-1} are given, and their corresponding $H_0^1(\Omega)$ and $L^2(\Omega)$ norms are bounded uniformly in h. To construct the iteration scheme, we use $(4.1)_2$ to rewrite the ion-transport equation $(4.1)_1$ as

$$(u_h^n - u_h^{n-1}, \phi_h) + \tau(\nabla u_h^n, \nabla \phi_h) - \tau(\mathbf{q}_h u_h^n, \nabla \phi_h) + \tau(r(u_h^n) - H_\delta(v_h^{n-1}), \phi_h) = 0, \quad (4.2)$$

for all $\phi_h \in \mathcal{U}_h$. Note that this equation is decoupled from $(4.1)_2$.

Before introducing the fixed point iteration we define the H^1-equivalent norm

$$|||u|||^2 := \|u\|^2 + \frac{2\tau}{2 + \tau L_r} \|\nabla u\|^2,$$

for which contraction will be obtained. Recall that L_r is the Lipschitz constant of the precipitation term $r(\cdot)$. We define the mapping $\mathcal{T}$

$$u_{i-1} \mapsto u_i = \mathcal{T} u_{i-1}$$

where i is the iteration index and for all $\phi_h \in \mathcal{U}_h$, u_i satisfies

$$(u_i, \phi_h) + \tau(\nabla u_i, \nabla \phi_h) - \tau(\mathbf{q}_h u_i, \nabla \phi_h) + \tau L_r(u_i, \phi_h)$$
$$= \tau L_r(u_{i-1}, \phi_h) - \tau(r(u_{i-1}), \phi_h) + (u_h^{n-1}, \phi_h) + \tau(H_\delta(v_h^{n-1}), \phi_h). \quad (4.3)$$

A good starting point for the iteration is $u_0 = u_h^{n-1}$. We have suppressed the superscript n in the iteration for the sake of presentation. In the iterative scheme considered here, we note that a fixed point of $\mathcal{T}$ satisfies (4.2), as the terms involving L_r gets canceled. Thus, in case of convergence, the limit of u_i is indeed a solution to (4.3). The problem of proving existence and uniqueness of solution of problem $\mathbf{P}_h^n$ is, thus, tantamount to

proving that of the fixed point of (4.3). This will be achieved by showing that $\mathcal{T}$ is a contraction. We mention that such constructions are common; we refer to [37,48] and the references therein for similar schemes.

Now we can prove the following result for the mapping $\mathcal{T}$:

Lemma 4.1 *$\mathcal{T}$ is a contraction map with respect to the $|||\cdot|||$ norm.*

Proof Recalling the assumptions on $\mathbf{q}_h$ in Sect. 2.1 we note that standard Lax–Milgram arguments ensure that $\mathcal{T}$ maps $\mathcal{U}_h$ into itself. Next, we show that $\mathcal{T}$ is a contraction. In this sense, with $u_{i-1,a}, u_{i-1,b} \in \mathcal{K}$ we define $u_{i,\alpha} = \mathcal{T}u_{i-1,\alpha}$ $(\alpha = a, b)$ and the differences

$$e_i := u_{i,a} - u_{i,b}, \quad \text{and} \quad e_{i-1} = u_{i-1,a} - u_{i-1,b}.$$

Subtracting (4.3) for $u_{i-1,b}$ from the one for $u_{i-1,a}$ gives

$$\begin{aligned}(e_i, \phi_h) + \tau(\nabla e_i, \nabla\phi_h) - \tau(\mathbf{q}_h e_i, \nabla\phi_h) + \tau L_r(e_i, \phi_h)\\ = \tau L_r(e_{i-1}, \phi_h) - \tau(r(u_{i-1,a}) - r(u_{i-1,b}), \phi_h).\end{aligned} \tag{4.4}$$

Choosing $\phi_h = e_i$, we obtain

$$(1+\tau L_r)\|e_i\|^2+\tau\|\nabla e_i\|^2-\tau(\mathbf{q}_h e_i, \nabla e_i) = \tau(L_r e_{i-1}-r(u_{i-1,a})+r(u_{i-1,b}), e_i). \tag{4.5}$$

Since r is Lipschitz continuous, we use mean value theorem to obtain

$$(1 + \tau L_r)\|e_i\|^2 + \tau\|\nabla e_i\|^2 - \tau(\mathbf{q}_h e_i, \nabla e_i) = \tau(L_r e_{i-1} - r'(\xi)e_{i-1}, e_i) \tag{4.6}$$

for some function ξ bounded by $u_{i-1,a}$ and $u_{i-1,b}$. Also note that the convection term vanishes as $\mathbf{q}_h$ is assumed divergence free. Since $0 \le L_r - r'(\xi) \le L_r$, the right hand side of (4.6) can be estimated as

$$(1 + \tau L_r)\|e_i\|^2 + \tau\|\nabla e_i\|^2 \le \tau L_r\|e_{i-1}\|\|e_i\| \le \frac{1}{2}\tau L_r\left(\|e_i\|^2 + \|e_{i-1}\|^2\right).$$

With $\gamma = \frac{\tau L_r}{2+\tau L_r} < 1$, this gives

$$\|e_i\|^2 + \frac{\tau}{1 + \frac{1}{2}\tau L_r}\|\nabla e_i\|^2 \le \frac{1}{2}\frac{\tau L_r}{1 + \frac{1}{2}\tau L_r}\|e_{i-1}\|^2 \le \gamma|||e_{i-1}|||^2,$$

showing that $\mathcal{T}$ is a contraction and thus has a unique fixed point (by Banach's Fixed Point Theorem). □

The above lemma shows that u_i converges to the fixed point of (4.2) as $i \nearrow \infty$. Clearly, its limit u_h^n satisfies (4.1). Having obtained it, computing v_h^n is straightforward. In other words we proved

Lemma 4.2 *Problem $\mathbf{P}_h^n$ has a unique solution (u_h^n, v_h^n).*

Remark 4.1 The numerical scheme presented here has a linear convergence rate (in the H^1 norm). This is lower than, e.g. the rate of Newton's iteration, which converges quadratically. This drawback is compensated by the fact that the convergence is guaranteed for any choice of parameters and for any starting point. The error converges to 0 as the iteration index approaches ∞. In practice, however, only 3–4 iterations are sufficient for a good approximation. Further, one expects a faster convergence in the L^2 norm since no τ factor is multiplying the L^2 norm in the H^1 equivalent norm $|||\ |||$ defined above, whereas the contraction constant γ for the mapping $\mathcal{T}$ approaches 0 with τ. We have not investigated the stability in time of this iteration process. Clearly, at each time step, an error is accumulated as the iteration procedure is ended in a finite number of steps. As in [37], Lemma 3.6, it can be shown that the accumulated error vanishes as τ tends to 0. We do not prove a similar result in this section since the goal is to show the existence and uniqueness of the solution for the discrete problem $\mathbf{P}_h^n$.

4.2 Stability estimates

Given the existence and uniqueness of solutions for the fully discrete problems $\mathbf{P}_h^n$, we proceed with energy estimates, which are similar to those obtained in Sect. 3:

Lemma 4.3 *There exists a $C > 0$ independent of τ, h and δ such that the following estimates hold*

$$\max_{k=1,\dots,N} \|u_h^k\| + \max_{k=1,\dots,N} \|v_h^k\| \le C, \tag{4.7}$$

$$\max_{k=1,\dots,N} \|v_h^k - v_h^{k-1}\| + \sum_{n=1}^{N} \|u_h^n - u_h^{n-1}\|^2 \le C\tau, \tag{4.8}$$

$$\sum_{n=1}^{N} \|\nabla(u_h^n - u_h^{n-1})\|^2 + \tau \sum_{n=1}^{N} \|\nabla u_h^n\|^2 \le C. \tag{4.9}$$

Proof The above estimates are obtained as in Lemma 3.5, with one exception: one cannot obtain the maximum principle as in the continuous case, as the corresponding (positive/negative cuts) test functions may not be admissible. Therefore we start by taking $\phi_h = u_h^n$ in $(4.1)_1$ and use $(4.1)_2$ to replace the last term in the resulting, which gives

$$(u_h^n - u_h^{n-1}, u_h^n) + \tau(\nabla u_h^n, \nabla u_h^n) + \tau(r(u_h^n), u_h^n) - \tau(\mathbf{q}_h u_h^n, \nabla u_h^n) + \tau(H_\delta(v_h^{n-1}), u_h^n) = 0.$$

For the first term one uses the identity

$$(u_h^n - u_h^{n-1}, u_h^n) = \frac{1}{2}\left(\|u_h^n\|^2 - \|u_h^{n-1}\|^2 + \|u_h^n - u_h^{n-1}\|^2\right), \tag{4.10}$$

which, combined with the Cauchy–Schwarz inequality gives

$$\begin{aligned} &\frac{1}{2}\left(\|u_h^n\|^2 - \|u_h^{n-1}\|^2 + \|u_h^n - u_h^{n-1}\|^2\right) + \frac{1}{2}\tau\|\nabla u_h^n\|^2 + \tau L_r\|u_h^n\|^2 \\ &\quad \le \frac{1}{2}\tau M_q\|u_h^n\|^2 + C\tau + \frac{1}{2}\tau\|u_h^n\|^2. \end{aligned}$$

Summing over $n = 1, \ldots, k$ (with $k \in \{1, \ldots, N\}$ arbitrarily) gives

$$\frac{1}{2}\|u_h^k\|^2 + \frac{1}{2}\sum_{n=1}^{k}\|u_h^n - u_h^{n-1}\|^2 + \frac{1}{2}\tau\sum_{n=1}^{k}\|\nabla u_h^n\|^2 + L_r\tau\sum_{n=1}^{k}\|u_h^n\|^2$$
$$\leq C\tau\sum_{n=1}^{k}\|u_h^n\|^2 + C. \tag{4.11}$$

The Discrete Gronwall Lemma provides now the first part in (4.7),

$$\sup_{k=1,\ldots,N}\|u_h^k\|^2 \leq C,$$

implying straightforwardly the second part of (4.9),

$$\tau\sum_{n=1}^{N}\|\nabla u_h^n\|^2 \leq C.$$

We continue with the first part in (4.8). With $\theta = v_h^n - v_h^{n-1}$ in $(4.1)_2$ and applying Cauchy–Schwarz inequality for the right hand side gives

$$\left\|v_h^n - v_h^{n-1}\right\|^2 \leq \tau\left\|r(u_h^n)\right\|\left\|v_h^n - v_h^{n-1}\right\| + \tau\left\|H_\delta(v_h^{n-1})\right\|\left\|v_h^n - v_h^{n-1}\right\|.$$

Using the estimate in (4.7) for u_h^n and the properties of r and H_δ immediately gives the desired estimate. To prove the second part in (4.7), we choose $\theta = v_h^n$ in $(4.1)_2$, proceed as in (4.10) for u_h^n to obtain

$$\frac{1}{2}\left(\|v_h^n\|^2 - \|v_h^{n-1}\|^2 + \|v_h^n - v_h^{n-1}\|^2\right) = \tau(r(u_h^n), v_h^n) - \tau(H_\delta(v_h^{n-1}), v_h^n). \tag{4.12}$$

The last term on the right rewrites

$$\left(H_\delta(v_h^{n-1}), v_h^n\right) = \left(H_\delta(v_h^{n-1}), v_h^{n-1}\right) - \left(H_\delta(v_h^{n-1}), v_h^{n-1} - v_h^n\right).$$

Using this into (4.12), multiplying the resulting by 2, and using the properties of H_δ (giving $(H_\delta(v_h^{n-1}), v_h^{n-1}) \geq 0$) and the Cauchy–Schwarz inequality gets

$$\left\|v_h^n\right\|^2 - \left\|v_h^{n-1}\right\|^2 + \left\|v_h^n - v_h^{n-1}\right\|^2 \leq 2\tau C\left\|u_h^n\right\|\left\|v_h^n\right\| + 2\tau\left(H_\delta(v_h^{n-1}), v_h^n - v_h^{n-1}\right).$$

Using further Young's inequality for the terms on the right and summing over $n = 1, \ldots, k$ (with $k \in \{1, \ldots, N\}$) gives

$$\left\|v_h^k\right\|^2 + \frac{1}{2}\sum_{n=1}^{k}\left\|v_h^n - v_h^{n-1}\right\|^2 \le \|v_I\|^2 + C\tau\sum_{n=1}^{k}\left\|v_h^n\right\|^2 + C\tau\sum_{n=1}^{k}\left\|u_h^n\right\|^2 + \sum_{n=1}^{k}2\tau^2\|H_\delta\|^2 \le \tau\sum_{n=1}^{k}\left\|v_h^n\right\|^2 + C + C\tau.$$

Using the bounds on u_h^n and on initial data and the Discrete Gronwall Lemma concludes (4.7).

The remaining estimates in (4.8) and (4.9) follow from the steps in the proof of (3.6) and (3.7); details are omitted. □

4.3 The convergence

As in the semi-discrete case, we consider the sequence of time discrete (u_h^n, v_h^n, w_h^n) solving problem $\mathbf{P}_h^n$, and construct a time continuous approximation by taking linear interpolation in time. We define,

$$\begin{aligned} U_h^\tau(t) &:= u_h^n\frac{(t-t_{n-1})}{\tau} + u_h^{n-1}\frac{(t_n-t)}{\tau}, \\ V_h^\tau(t) &:= v_h^n\frac{(t-t_{n-1})}{\tau} + v_h^{n-1}\frac{(t_n-t)}{\tau}, \\ W_h^\tau(t) &:= H_\delta(V_h^\tau(t)), \end{aligned} \tag{4.13}$$

and use compactness arguments for time-continuous triples $(U_h^\tau, V_h^\tau, W_h^\tau)$ to identify limit triples and the system that these limit points satisfy. In this sense, using estimates (4.8–4.9) one straightforwardly proves (we omit the details)

Lemma 4.4 *A constant C independent of τ, δ or h exists s.t.*

$$\|U_h^\tau\|^2 + \|V_h^\tau\|^2 \le C, \tag{4.14}$$

$$\|\partial_t U_h^\tau\|^2 + \|\nabla U_h^\tau\|^2 + \|\partial_t V_h^\tau\|^2 \le C, \tag{4.15}$$

$$0 \le W_h^\tau \le 1, \tag{4.16}$$

where the norms are taken in $L^2(0,T;L^2(\Omega))$.

In view of Lemma 4.4 one has

Lemma 4.5 *Along a sequence of pairs (τ, h) approaching $(0,0)$ and with $\delta = O(\sqrt{\tau})$, a limit triple $(u, v, w) \in \mathcal{U}\times\mathcal{V}\times\mathcal{W}$ exists s.t.*

1. *$U_h^\tau \rightharpoonup u$ weakly in $L^2((0,T);H_0^1(\Omega))$,*
2. *$\partial_t U_h^\tau \rightharpoonup \partial_t u$ weakly in $L^2((0,T);L^2(\Omega))$,*
3. *$V_h^\tau \rightharpoonup v$ weakly in $L^2((0,T);L^2(\Omega))$,*
4. *$\partial_t V_h^\tau \rightharpoonup \partial_t v$ weakly in $L^2((0,T);L^2(\Omega))$,*
5. *$W_h^\tau \rightharpoonup w$ weakly-star in $L^\infty(\Omega)$.*

As in Sect. 3, it remains to prove that the limit triple is a weak solution in the sense of Definition 2.1. In this respect, to identify the limit object for the dissolution term, we use again the strong convergence of V_h^τ. This is proved in the semi-discrete case by translation estimates, which can not be applied straightforwardly in the fully discrete situation as a translation of the test functions may leave the space $\mathcal{U}_h$. This is due to the fact that the translations are not remaining within the same triangle. Therefore we prove the strong convergence by employing ideas from [35]. In this context, we use the higher regularity of v_I. We start with

Proposition 4.6 *Let Π be the interpolation operator that maps $H^1(\Omega) \cap C(\bar{\Omega})$ to the space $\mathcal{U}_h$. Further, let $g : \mathbb{R} \mapsto \mathbb{R}$ be a Lipschitz function with the Lipschitz constant L_g, and $f : \Omega \mapsto \mathbb{R}$ be defined by $f = g(u)$. Then for any $u \in \mathcal{U}_h$ it holds that*

$$\|\nabla \Pi f\| \leq L_g \|\nabla u\|. \tag{4.17}$$

Proof The proof follows the calculations in [35] (pp. 469; also see [49]), therefore it is only sketched here briefly. First note that f is an H^1 function. With $A_i^T = (x_i, y_i)$ denoting the vertices of the triangle T ($i = 1, 2,$ or 3), since Πf is piecewise linear it holds

$$\Pi f = \sum_{i=1}^{3} (a_i^T x + b_i^T y + c_i^T) \Pi f(A_i^T), \quad \text{with}$$

$$a_i^T = \frac{1}{2|T|}(y_j - y_k), \quad b_i^T = \frac{1}{2|T|}(x_k - x_j), \quad \text{and} \quad c_i^T = \frac{1}{2|T|}(x_j y_k - x_k y_j).$$

Here the indices i, j, k are permuted cyclically and $|T|$ represents the area of the triangle T. In the present context, equation (2.5) in [35] rewrites as

$$\|\nabla \Pi f\|^2 = \sum_{T \in \mathcal{T}_h} \frac{1}{4|T|} \left\{ (A_k^T A_i^T, A_k^T A_j^T) |f(A_i^T) - f(A_j^T)|^2 \right\},$$

where $A_k^T A_i^T$ is a vector connecting the vertex i to the vertex k in the triangle T. Using the Lipschitz continuity of g, this gives

$$\|\nabla \Pi f\|^2 \leq L_g^2 \sum_{T \in \mathcal{T}_h} \frac{1}{4|T|} \{ (A_k^T A_i^T, A_k^T A_j^T) |u(A_i^T) - u(A_j^T)|^2 \} = L_g^2 \|\nabla u\|^2,$$

which is exactly the conclusion in the proposition. □

Remark 4.2 It is important to note that the constant in Proposition 4.6 is exactly L_g, the Lipschitz constant of g. This is needed in the proof of the next lemma.

Lemma 4.7 *If $v_I \in H^1(\Omega)$, along the sequence $(\tau, h) \searrow (0, 0)$ considered in Lemma 4.5 one has*

$$V_h^\tau \to v \quad \textit{strongly in} \quad L^2(0, T; L^2(\Omega)). \tag{4.18}$$

Proof From $(4.1)_2$, for all $\theta_h \in \mathcal{U}_h$ it holds

$$\left(v_h^n - v_h^{n-1}, \theta_h\right) = \tau \left(r(u_h^n) - H_\delta(v_h^{n-1}), \theta_h\right).$$

Since v_h^n and v_h^{n-1} are in $\mathcal{P}_1$, within each triangle T this gives

$$\nabla v_h^n = \tau \nabla \Pi r(u_h^n) - \nabla \Pi \left(v_h^{n-1} - \tau H_\delta(v_h^{n-1})\right). \tag{4.19}$$

Next, note that $g(v) = v - \tau H_\delta(v)$ is Lipschitz continuous with the Lipschitz constant $1 - \frac{\tau}{\delta}$. By Proposition 4.6, we have

$$\|\nabla \Pi(v_h^{n-1} - \tau H_\delta(v_h^{n-1}))\| \le \left(1 - \frac{\tau}{\delta}\right) \|\nabla v_h^{n-1}\| \le \|\nabla v_h^{n-1}\|$$

whenever $\tau < \delta$, which is satisfied if choosing $\delta = O(\sqrt{\tau})$. Using this into (4.19), this gives

$$\|\nabla v_h^n\| - \|\nabla v_h^{n-1}\| \le \tau L_r \|\nabla u_h^n\|.$$

Summing over $n = 1, \ldots, k$ (for any $k \in \{1, \ldots, N\}$) we obtain

$$\|\nabla v_h^k\| \le \|\nabla v_I\| + \sum_{n=1}^{k} \tau L_r \|\nabla u_h^n\|,$$

which actually proves that

$$\sup_{k=1,\ldots,N} \|\nabla v_h^k\| \le C. \tag{4.20}$$

Recalling the definition of V_h^τ, we have

$$\int_0^T \int_\Omega |\nabla V_h^\tau|^2 dx dt \le C,$$

uniformly w.r.t. τ, h and δ.

As $\partial_t V_h^\tau$ is also bounded uniformly in $L^2(0, T; L^2(\Omega))$ we obtain the strong convergence of V_h^τ in $L^2(0, T; L^2(\Omega))$. □

4.4 The limit equations

Finally we investigate the limit of $(U_h^\tau, V_h^\tau, W_h^\tau)$. We have

Theorem 4.8 *The limit (u, v, w) in Lemma 4.5 is a weak solution in the sense of Definition 2.1.*

Proof For any $\phi \in L^2(0,T;H_0^1(\Omega))$ we consider $\phi_h = P_h\phi$ [the projection of ϕ defined in (2.5)]. By $(4.1)_1$, (U_h^τ, V_h^τ) satisfies

$$\begin{aligned}
&\int_0^T (\partial_t U_h^\tau, \phi)dt + \int_0^T (\nabla U_h^\tau, \nabla\phi)dt + \int_0^T (\mathbf{q}_h \cdot \nabla U_h^\tau, \phi)dt + \int_0^T (\partial_t V_h^\tau, \phi)dt \\
&= \sum_{n=1}^N \int_{t_{n-1}}^{t_n} (\partial_t V_h^\tau, \phi - \phi_h) + \sum_{n=1}^N \int_{t_{n-1}}^{t_n} (\partial_t U_h^\tau, \phi - \phi_h)dt \\
&\quad + \sum_{n=1}^N \int_{t_{n-1}}^{t_n} (\nabla U_h^\tau, \nabla(\phi - \phi_h))dt + \sum_{n=1}^N \int_{t_{n-1}}^{t_n} ((\nabla U_h^\tau - \nabla u_h^n), \nabla\phi_h)dt \\
&\quad - \sum_{n=1}^N \int_{t_{n-1}}^{t_n} (\mathbf{q}_h U_h^\tau, (\nabla\phi - \nabla\phi_h))dt - \sum_{n=1}^N \int_{t_{n-1}}^{t_n} (\mathbf{q}_h(U_h^\tau - u_h^n), \nabla\phi_h)dt. \qquad (4.21)
\end{aligned}$$

We proceed by showing that the terms on the right are vanishing as the discretization parameters h and τ are approaching 0. To this aim we first take test functions that are H^2 in space, i.e. $\phi \in L^2(0,T;H_0^2(\Omega))$. As will be seen below, this extra regularity allows controlling terms involving $\nabla(\phi - \phi_h)$. By this we prove that (u, v) satisfy $(2.7)_1$, but only for test functions having a better regularity in space. Once this is established, density arguments ensure that the equality is satisfied also for test functions in $L^2(0,T;H_0^1(\Omega))$.

By Lemma 4.5, all terms on the left hand side converge to the desired limits. This is obvious in the first two terms. For the third one we recall the assumption on $\mathbf{q}_h$ and $\mathbf{q}$, namely that $\mathbf{q}_h - \mathbf{q} \in L^\infty(\Omega)$ and, moreover, that $\mathbf{q}_h$ converges strongly to $\mathbf{q}$ in $L^2(\Omega)$. Combined with the weak convergence of ∇U_h^τ, one immediately gets that

$$\int_0^T (\mathbf{q}_h \cdot \nabla U_h^\tau, \phi)dt \to \int_0^T (\mathbf{q} \cdot \nabla u, \phi)dt. \qquad (4.22)$$

It only remains to show that the right hand side of (4.21) vanishes in the limit. We treat these terms, denoted by $\mathcal{I}_1, \ldots, \mathcal{I}_6$ separately. First, as $h \searrow 0$ we have

$$|\mathcal{I}_1| \le \left(\int_0^T \|\partial_t V_h^n\|^2 dt\right)^{\frac{1}{2}} \left(\sum_{n=1}^N \int_{t_{n-1}}^{t_n} \|\phi - \phi_h\|^2 dt\right)^{\frac{1}{2}} \le Ch\|\nabla\phi\|_{L^2(0,T;L^2(\Omega))} \to 0.$$

For $\mathcal{I}_2$ and $\mathcal{I}_3$ the arguments are similar. For example, since $\phi \in L^2(0,T;H_0^2(\Omega))$ one has $\|\nabla(\phi - \phi_h)\| \le Ch\|\phi\|_{H_0^2(\Omega)}$. With $h \searrow 0$,

$$|\mathcal{I}_3| \leq \left(\int_0^T \|\nabla U_h^\tau\|^2 dt \right)^{\frac{1}{2}} \left(\sum_{n=1}^N \int_{t_{n-1}}^{t_n} \|\nabla(\phi - \phi_h)\|^2 dt \right)^{\frac{1}{2}} \leq Ch\|\phi\|_{L^2(0,T;H_0^2(\Omega))} \to 0.$$

For $\mathcal{I}_4$ we use (4.9) to obtain (for $\tau \searrow 0$)

$$|\mathcal{I}_4| \leq \left(\sum_{n=1}^N \tau \|\nabla u_h^n - \nabla u_h^{n-1}\|^2 \right)^{\frac{1}{2}} \left(\sum_{n=1}^N \tau \|\nabla \phi_h\|^2 \right)^{\frac{1}{2}} \to 0.$$

For $\mathcal{I}_5$ we proceed as for $\mathcal{I}_3$,

$$|\mathcal{I}_5| \leq \left(\int_0^T \|\mathbf{q}_h U_h^\tau\|^2 dt \right)^{\frac{1}{2}} \left(\sum_{n=1}^N \int_{t_{n-1}}^{t_n} \|\nabla(\phi - \phi_h)\|^2 dt \right)^{\frac{1}{2}} \leq Ch\|\phi\|_{L^2(0,T;H_0^2(\Omega))}.$$

To conclude with the first equation, for $\mathcal{I}_6$ we use (4.8) to obtain

$$|\mathcal{I}_6| \leq M_q \left(\sum_{n=1}^N \tau \|u_h^n - u_h^{n-1}\|^2 dt \right)^{\frac{1}{2}} \left(\sum_{n=1}^N \tau \|\nabla \phi_h\|^2 dt \right)^{\frac{1}{2}} \to 0.$$

Concerning the second equation in (2.7), by $(4.1)_2$ we have

$$\begin{aligned}
&\int_0^T (\partial_t V_h^\tau, \theta) dt - \int_0^T (r(U_h^\tau) - W_h^\tau, \theta) dt \\
&= \sum_{n=1}^N \int_{t_{n-1}}^{t_n} (\partial_t V_h^\tau, \theta - \theta_h) dt + \sum_{n=1}^N \int_{t_{n-1}}^{t_n} (r(u_h^n) - r(U_h^\tau), \theta_h) dt \\
&\quad + \sum_{n=1}^N \int_{t_{n-1}}^{t_n} (r(U_h^\tau), \theta_h - \theta) dt + \sum_{n=1}^N \int_{t_{n-1}}^{t_n} (W_h^\tau - H_\delta(v_h^{n-1}), \theta_h) dt \\
&\quad + \sum_{n=1}^N \int_{t_{n-1}}^{t_n} (W_h^\tau, \theta - \theta_h) dt, \qquad (4.23)
\end{aligned}$$

for all $\theta \in L^2(0, T; H_0^1(\Omega))$, and with $\theta_h = P_h\theta$. Recall that (see [42])

$$\|\theta - \theta_h\| \leq Ch\|\nabla\theta\|. \qquad (4.24)$$

The desired limit equations are retrieved once it is proved that the integrals on the right hand side, denoted by $\mathcal{J}_1, \ldots, \mathcal{J}_5$, are vanishing as τ and h are approaching 0. For $\mathcal{J}_1$ we get

$$|\mathcal{J}_1| \leq \left(\int_0^T \|\partial_t V_h^\tau\|^2 dt \right)^{\frac{1}{2}} \left(\sum_{n=1}^N \int_{t_{n-1}}^{t_n} \|(\theta - \theta_h)\|^2 dt \right)^{\frac{1}{2}} \leq Ch \|\theta\|_{L^2(0,T;H_0^1(\Omega))},$$

which vanishes in the limit as $h \searrow 0$. Next, we use (4.8) to obtain

$$|\mathcal{J}_2| \leq \left(\sum_{n=1}^N \tau L_r^2 \|u_h^n - u_h^{n-1}\|^2 \right)^{\frac{1}{2}} \left(\sum_{n=1}^N \tau \|\theta_h\|^2 \right)^{\frac{1}{2}} \to 0.$$

For $\mathcal{J}_3$ one has

$$|\mathcal{J}_3| \leq L_r \left(\int_0^T \|U_h^\tau\|^2 dt \right)^{\frac{1}{2}} \left(\sum_{n=1}^N \int_{t_{n-1}}^{t_n} \|(\theta - \theta_h)\|^2 dt \right)^{\frac{1}{2}} \leq Ch \|\theta\|_{L^2(0,T;H_0^1(\Omega))} \to 0.$$

Further, for $\mathcal{J}_4$, we use the definition of W_h^τ, the Lipschitz continuity of H_δ and (4.8) to obtain

$$|\mathcal{J}_4| \leq \sum_{n=1}^N \tau \frac{1}{\delta} \|v_h^n - v_h^{n-1}\| \|\theta_h\| \leq C \frac{\tau^2}{\delta} \sum_{n=1}^N \|\theta_h\|.$$

Since δ is chosen s.t. $\tau/\delta \to 0$ we obtain that $\mathcal{J}_4$ vanishes too.

Finally, due to (4.24), as $h \searrow 0$ we have

$$|\mathcal{J}_5| \leq C \left(\sum_{n=1}^N \int_{t_{n-1}}^{t_n} \|\theta - \theta_h\|^2 dt \right)^{\frac{1}{2}} \leq Ch \|\nabla\theta\|_{L^2(0,T;L^2(\Omega))} \to 0.$$

By this we have shown that the terms on the right in (4.23) are all vanishing.

The final step is to prove that $w \in H(v)$, with the choice stated in Definition 2.1. For this, the arguments are exactly the ones in Theorem 3.10, therefore we do not repeat them here. Having this we note that the limit triple (u, v, w) indeed satisfies (2.7), but for test functions having a spatial regularity that is better than stated in the definition of the weak solution: $\phi \in L^2(0, T; H_0^2(\Omega))$ and $\theta \in L^2(0, T; H_0^1(\Omega))$. In view of the regularity of u and v, density arguments can be employed to show that the limit equations also hold for $\phi \in L^2(0, T; H_0^1(\Omega))$ and $\theta \in L^2(0, T; L^2(\Omega))$, which completes the proof. □

5 Numerical experiments

We carry out numerical experiments for different situations. The scheme is validated on a 1D situation where we study the concentration profile and the dissolution fronts.

With $\Omega = (0, 1)$, $D = 1e-2$, $r(u) = u$, $\mathbf{q} = 1$, the following boundary conditions are imposed: $u = 0$ at $x = 0$; and $\frac{\partial u}{\partial x} = 0$ at $x = 1$. Initially we take $u_I = 1$ and $v_I = 0.2$ for all $x \in [0, 1]$. Note that for the initial conditions above one has $r(u_I) - H(v_I) = 0$, and therefore in the beginning the system is in equilibrium: the dissolution and precipitation processes balance each other. Without any perturbation (through the boundary data), the situation would remain in equilibrium (i.e. $u = 1$ and $v = 0.2$ for all times and at any location). However, this equilibrium is disturbed at $x = 0$ because of the boundary condition $u = 0$. This leads to the initiation of the dissolution process, which takes place as t increases. Also note that after some time (called t_s), the entire precipitate at $x = 0$ is being dissolved: $v(t_s, 0) = 0$. Since $u(t, 0) = 0$, this allows an easy calculation of t_s:

$$0 - v_I = \int_0^{t_s} \partial_t v(t, 0) dt = \int_0^{t_s} (u - H(v))(t, 0) dt = -t_s, \quad \text{thus } t_s = v_I = 0.2.$$

Computations are performed for $t \in (0, 1]$ and the discretization in space is obtained on a regular grid of size $h = 1e-3$. Further, we choose standard first order upwinding for the transport term. For the time discretization, we choose $\tau = 1e-3$ and we use regularized Heaviside function (3.1) for the dissolution rate for the 1D problem. For the regularization parameter δ, we choose $\delta = 0.1(\tau^{0.5})$.

The profiles of the solute u and of the precipitate v at different times are presented in Fig. 1. As expected, the dissolution is stronger at the inflow $x = 0$; after t_s, two regions can be identified in the domain Ω: precipitate is present only for x larger than a value x_s depending on the time t, $x_s = x_s(t)$. For $x \in (0, x_s(t))$ one has $v(t, x) = 0$, whereas $v(t, x) > 0$ for $x > x_s(t)$. This situation is assimilated in [9,10] with a dissolution front propagating rightwards (with the flow); its location $x_s(t)$ is a free boundary separating the two aforementioned regions (see [11]). There two quantities of interest are identified: the speed of the dissolution front Q_v given by (see Proposition 1.2 of [10])

$$Q_v = q \frac{u^*}{u^* + v_I} \approx 0.833,$$

and the "waiting time" at which the dissolution front has appeared: $t_s = 0.2$ (as computed above). These two information are contained in defining the free boundary x_s

$$x_s(t) := \sup\{x \in (0, L) : v(\cdot, t) = 0 \text{ a.e. in } (0, x)\}.$$

The evolution of $x_s(t)$ is presented in Fig. 2. Note that the numerically computed values for the time t_s (when a complete dissolution is encountered at $x = 0$) and the slope of the graph of x_s for $t > t_s$ (which is similar to the velocity of the dissolution front/free boundary) are in good agreement with the values predicted theoretically. Here we obtain: $t_s = 0.199$ and $Q_v = 0.8464$. These numerical results, together with the qualitative behavior of the numerical solution, which is again in agreement with the theory in [9–11], provide a validation for the numerical scheme proposed here.

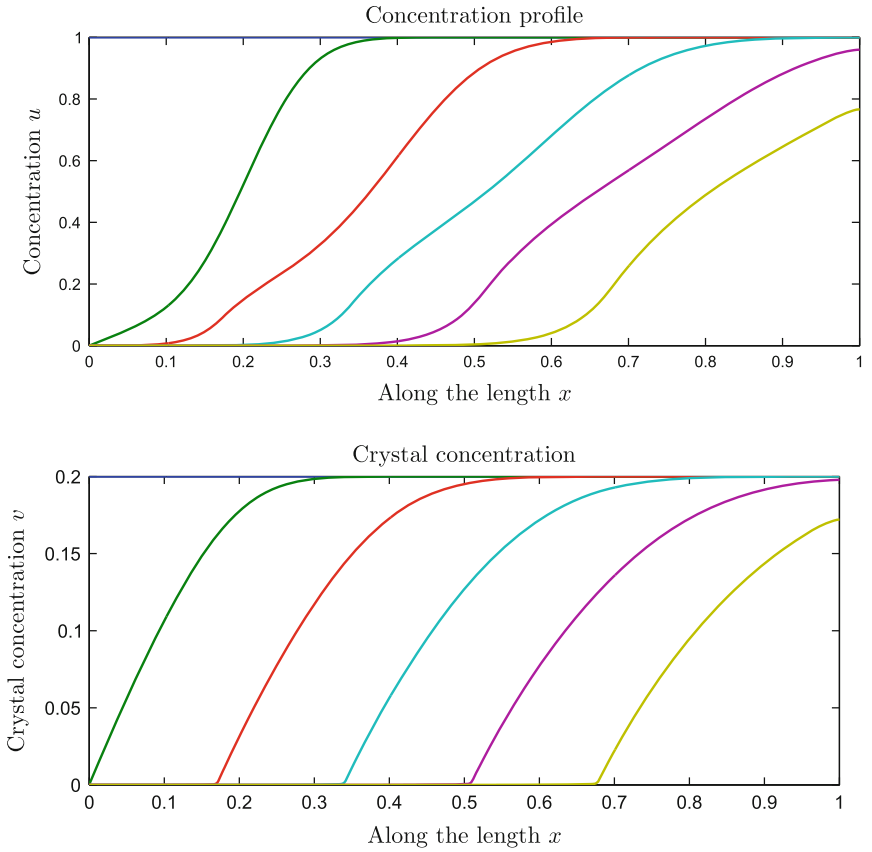

Fig. 1 Concentration profiles for u and v at different times: $t = 0, 0.2, 0.4, 0.6, 0.8, 1$ (from *left* to *right*). Note that v is a dissolution front moving rightwards as t increases. The dissolution effects are also visible for u

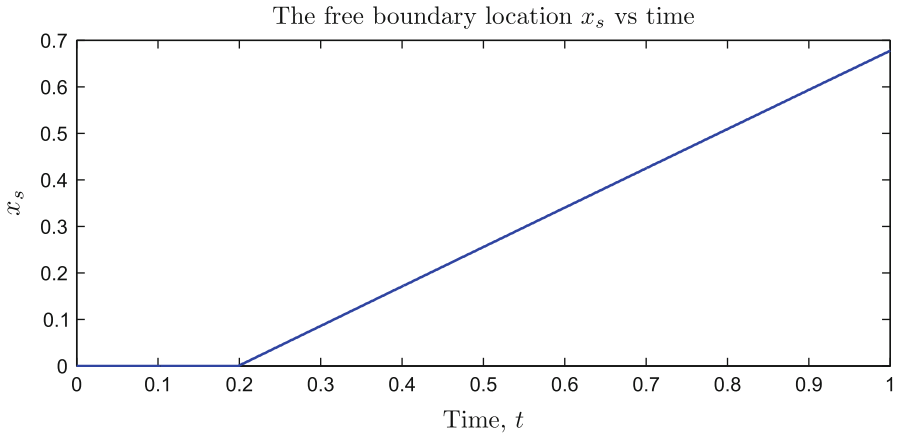

Fig. 2 The free boundary location, x_s. Note the starting time $t_s = 0.2$ for the beginning of the dissolution front. Also, the slope of the free boundary is equal to Q_v

5.1 Two-dimensional examples

Now we choose $\Omega = (0, 1) \times (0, 1)$ and further

$$T = 1,\ \mathbf{q} = (0.5, 0),\ D = 1,\ r(u) = 2u_+(u - 0.5)_+;$$
$$h = 0.1,\ \tau = 1e - 3,\ \delta = 0.2\sqrt{\tau},$$

where $[u]_+ := \max\{0, u\}$. No diffusive flow is assumed on all boundaries condition except at the inflow $x = 0$, $-v \cdot \nabla u = 0$ on $\Gamma \backslash \{x = 0\}$. The boundary condition at $x = 0$ is specified in the two different cases considered below. Note that for this choice of precipitation rate, $r(u) = 0$ for $u \leq 0.5$ and $r(1) = 1$ so that $u = 1$ is the equilibrium solute concentration, when the dissolution rates balances the precipitation rate. To state the initial condition we also define $\Omega_v := (0.2, 0.8) \times (0.2, 0.8)$; clearly Ω_v is a square inside the original domain Ω. We study the following cases:

5.1.1 Equilibrium situation

We start with a trivial case, when according to the theory there should be no change in the concentration of solute or precipitate. For the initial conditions, we choose $u_I = 1,\ v_I = 0.1\chi_{\Omega_v}$ with χ_{Ω_v} denoting the characteristic function for the set Ω_v. We impose $u = 1$ at $x = 0$ as the boundary condition. Since $u = 1$ is the equilibrium concentration, the initial and the boundary conditions ensure that no changes take place in the solution as the initial conditions satisfy the Eqs. (2.1, 2.2). This is easily confirmed numerically by computing the $L^2(0, T; L^2(\Omega))$ norm of the difference between the numerical solution and the initial condition (viewed as constant in time):

$$\|u_I - u_h^n\| = 9.35 \times 10^{-4}, \quad \|v_I - v_h^n\| = 4.2 \times 10^{-3}.$$

5.1.2 Dissolution fronts

To initiate the dissolution front, we change the boundary condition at $x = 0$ by maintaining the same initial data:

$$u_I = 1,\ v_I = 0.1\chi_{\Omega_v},\ u = 0 \text{ at } x = 0.$$

Clearly, this leads to a decay of the solute concentration: $u < 1$ implies that $r(u) - H(v) < 0$, initiating a dissolution process. Numerically, as shown in Fig. 3, this process indeed takes place, leading to the depletion of the precipitate concentration with the domain $v > 0$ shrinking as time proceeds.

5.2 Convergence studies

We consider a test problem similar to (2.1, 2.2), but including a right hand side in the first equation. This is chosen in such a way that the problem has an exact solution (see [19] where a similar exact solution is proposed for test purposes), which is used

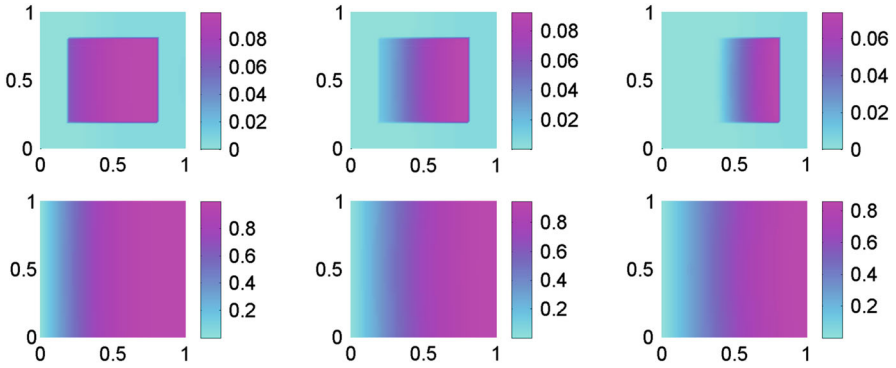

Fig. 3 Concentration profiles for the precipitate v (*top*) and solute u (*bottom*) at $t = 0.05, 0.1, 0.15$. Initially $v = 0.1$ in Ω_v and, as t increases, dissolution takes place. More dissolution is encountered on the left side than on the right side due to the boundary condition at $x = 0$. Also note that u decreases from its initial value 1 to the asymptotic value, $u = 0$

then to test the convergence of the conformal scheme. Specifically, for $T = 1$ and $\Omega = (0, 5) \times (0, 1)$, and with $r(u) = [u]_+^2$, we consider the problem

$$\begin{cases} \partial_t(u + v) + \nabla \cdot (\mathbf{q}u - \nabla u) = f, & \text{in } \Omega^T, \\ \partial_t v = (r(u) - w), & \text{on } \Omega^T, \\ w \in H(v), & \text{on } \Omega^T. \end{cases}$$

Here $\mathbf{q} = (1, 0)$ is a constant velocity, whereas

$$f(t, x, y) = \frac{1}{2} e^{x-t-5} \left(1 - e^{x-t-5}\right)^{-\frac{3}{2}} \left(1 - \frac{1}{2} e^{x-t-5}\right) - \begin{cases} 0, & \text{if } x < t, \\ e^{x-t-5}, & \text{if } x \geq t, \end{cases}$$

and the boundary and initial conditions are such that

$$u(t, x, y) = \left(1 - e^{x-t-5}\right)^{\frac{1}{2}} \quad \text{and} \quad v(t, x, y) = \begin{cases} 0, & \text{if } x < t, \\ \frac{e^{x-t}-1}{e^5} & \text{if } x \geq t, \end{cases}$$

$$\text{providing} \quad w(t, x, y) = \begin{cases} 1, & \text{if } x < t, \\ 1 - e^{x-t-5} & \text{if } x \geq t, \end{cases}$$

form the solution triple.

The simulations are carried out for a uniform mesh diameter h and time step $\tau = 0.2h$. Further, $\delta = 0.2\tau^{0.5}$ is the regularization parameter. We start with $h = 0.5$, and refine the mesh (and correspondingly τ and δ) four times successively by halving h up to $h = 0.03125$. We compute the errors for u and v in the $L^2(0, T; L^2(\Omega))$ norms,

$$E_u^h = \|u - U^\tau\|_{L^2(\Omega^T)}, \quad \text{respectively} \quad E_v^h = \|v - V^\tau\|_{L^2(\Omega^T)}.$$

These are presented in Table 1. Although theoretically no error estimates could be given due to the particular character of the dissolution rate, Table 1 also includes

Table 1 Convergence results, $h = 5\tau$ and $\delta = 0.2\sqrt{\tau}$

h	E_u^h	α	E_v^h	β
0.5	0.038		0.102	
0.25	0.0147	1.37	0.0539	0.92
0.125	0.0065	1.17	0.0355	0.60
0.0625	0.0034	0.93	0.0237	0.58
0.03125	0.0020	0.76	0.0158	0.58

an estimate of the convergence order, based on the reduction factor between two successive calculations:

$$\alpha = \log_2(E_u^h / E_u^{\frac{h}{2}}), \quad \text{and} \quad \beta = \log_2(E_v^h / E_v^{\frac{h}{2}}).$$

For this simple test case, the convergence is slightly worse than linear.

6 Conclusions and discussions

We have considered both semi-discrete and fully discrete schemes for the macroscale equations. For the fully discrete case, we consider linear finite elements on triangular meshes. These schemes have been analyzed for their convergence and the proof relies on stability estimates and the compactness arguments. To deal with the multi-valued dissolution rate, a regularization step is included. We obtain stability estimates that do not depend on the discretization or regularization parameters. The proofs for the semi-discrete and the fully discrete cases follow similar strategy, however, there are some important differences. Whereas the semi-discrete case retains the maximum principle, we have to rely on different estimates in the fully discrete case. Also, the translation estimates to obtain the strong convergence are easily applicable for the semi-discrete situation, but not for the fully discrete case. For the choice of basis functions taken here, that is, piecewise linear elements on a triangle, the usual method of obtaining pointwise estimates does not work in fully discrete case thereby not necessarily having the maximum principle. Next, instead of using the discrete analogue of translation estimates, the properties of Lagrangian interpolation operator on a triangle are used to obtain the strong convergence needed to deal with the nonlinearities.

The numerical experiments present several interesting aspects of the model. In the 1D case, we have shown the occurrence of dissolution fronts propagating forward. Further, we have plotted the free boundary location and its evolution in time. We find an excellent agreement with the theoretical predictions. For the 2D model, we have shown that the model remains in equilibrium whenever the initial and boundary values for the solute concentration are compatible with this equilibrium. Further, if the precipitate is present and the boundary conditions are determining the fluid to become undersaturated, we clearly see the dissolution processes taking place. Finally, we construct an exact solution and compare the numerical solution to study the convergence behavior.

Acknowledgments K. Kumar would like to thank the Technology Foundation STW for the financial support through the Project 07796, "Second Generation of Integrated Batteries". The authors are members of the International Research Training Group NUPUS funded by the German Research Foundation DFG (GRK 1398) and by the Netherlands Organisation for Scientific Research NWO (DN 81-754). Part of the work was carried out when K. Kumar visited the Institute of Mathematics, University of Bergen. The support is gratefully acknowledged. K. Kumar would also like to thank Dr. Thomas Wick and Dr. Ahmed El Sheikh (UT Austin) for their feedback on the numerical computations. F.A. Radu acknowledges the support of Statoil through the Akademia Grant 2012–2013.

References

1. Rubin, J.: Transport of reacting solutes in porous media: relation between mathematical nature of problem formulation and chemical nature of reaction. Water Resour. Res. **19**, 1231–1252 (1983)
2. Metzmacher, I., Radu, F.A., Bause, M., Knabner, P., Friess, W.: A model describing the effect of enzymatic degradation on drug release from collagen minirods. Eur. J. Pharm. Biopharm. **67**(2), 349–360 (2007)
3. Moszkowicz, P., Pousin, J., Sanchez, F.: Diffusion and dissolution in a reactive porous medium: mathematical modelling and numerical simulations. In: Proceedings of the Sixth International Congress on Computational and Applied Mathematics (Leuven, 1994), vol. 66, pp. 377–389 (1996)
4. Pawell, A., Krannich, K.-D.: Dissolution effects in transport in porous media. SIAM J. Appl. Math. **56**(1), 89–118 (1996)
5. Pousin, J.: Infinitely fast kinetics for dissolution and diffusion in open reactive systems. Nonlinear Anal. **39**(3, Ser. A: Theory Methods), 261–279 (2000)
6. Bouillard, N., Eymard, R., Herbin, R., Montarnal, P.: Diffusion with dissolution and precipitation in a porous medium: mathematical analysis and numerical approximation of a simplified model. M2AN. Math. Model. Numer. Anal. **41**(6), 975–1000 (2007)
7. Knabner, P., van Duijn, C.J., Hengst, S.: An analysis of crystal dissolution fronts in flows through porous media. Part 1: compatible boundary conditions. Adv. Water Resour. **18**, 171–185 (1995)
8. van Duijn, C.J., Knabner, P.: Solute transport through porous media with slow adsorption. In Free boundary problems: theory and applications, vol. I (Irsee, 1987). Pitman Res. Notes Math. Ser., vol. 185, pp. 375–388. Longman Sci. Tech., Harlow (1990)
9. van Duijn, C.J., Knabner, P.: Solute transport in porous media with equilibrium and nonequilibrium multiple-site adsorption: travelling waves. J. Reine Angew. Math. **415**, 1–49 (1991)
10. van Duijn, C.J., Knabner, P.: Travelling wave behaviour of crystal dissolution in porous media flow. Eur. J. Appl. Math. **8**(1), 49–72 (1997)
11. van Duijn, C.J., Pop, I.S.: Crystal dissolution and precipitation in porous media: pore scale analysis. J. Reine Angew. Math. **577**, 171–211 (2004)
12. van Noorden, T.L., Pop, I.S.: A Stefan problem modelling crystal dissolution and precipitation. IMA J. Appl. Math. **73**(2), 393–411 (2008)
13. Muntean, A., Böhm, M.: A moving-boundary problem for concrete carbonation: global existence and uniqueness of weak solutions. J. Math. Anal. Appl. **350**(1), 234–251 (2009)
14. Kumar, K., van Noorden, T.L., Pop, I.S.: Effective dispersion equations for reactive flows involving free boundaries at the microscale. Multiscale Model. Simul. **9**(1), 29–58 (2011)
15. van Noorden, T.L.: Crystal precipitation and dissolution in a thin strip. Eur. J. Appl. Math. **20**(1), 69–91 (2009)
16. Kumar, K., van Noorden, T.L., Pop, I.S.: Upscaling of reactive flows in domains with moving oscillating boundaries. Discrete Contin. Dyn. Sys. Ser. S **7**, 95–111 (2014)
17. van Noorden, T.L., Pop, I.S., Ebigbo, A., Helmig, R.: An upscaled model for biofilm growth in a thin strip. Water Resour. Res. **46**, W06505 (2010)
18. Ray, N., van Noorden, T.L., Radu, F.A., Friess, W., Knabner, P.: Drug release from collagen matrices including an evolving microstructure. Z. Angew. Math. Mech. **93**(10–11), 811–822 (2013). doi:10.1002/zamm.201200196
19. Kumar, K., Pop, I.S., Radu, F.A.: Numerical analysis for an upscaled model for dissolution and precipitation in porous media. In: Cangiani, Andrea, Davidchack, Ruslan L., Georgoulis, Emmanuil, Gorban, Alexander N., Levesley, Jeremy, Tretyakov, Michael V. (eds.) Numerical Mathematics and Advanced Applications 2011, pp. 703–711. Springer, Berlin (2013)

20. Barrett, J.W., Knabner, P.: Finite element approximation of the transport of reactive solutes in porous media. I. Error estimates for nonequilibrium adsorption processes. SIAM J. Numer. Anal. **34**(1), 201–227 (1997)
21. Barrett, J.W., Knabner, P.: Finite element approximation of the transport of reactive solutes in porous media. II. Error estimates for equilibrium adsorption processes. SIAM J. Numer. Anal. **34**(2), 455–479 (1997)
22. Radu, F.A., Pop, I.S.: Newton method for reactive solute transport with equilibrium sorption in porous media. J. Comput. Appl. Math. **234**(7), 2118–2127 (2010)
23. Radu, F.A., Pop, I.S.: Mixed finite element discretization and newton iteration for a reactive contaminant transport model with nonequilibrium sorption: convergence analysis and error estimates. Comput. Geosci. **15**, 431–450 (2011)
24. Radu, F.A., Pop, I.S., Attinger, S.: Analysis of an Euler implicit-mixed finite element scheme for reactive solute transport in porous media. Numer. Methods Partial Differ. Equ. **26**(2), 320–344 (2010)
25. Radu, F.A., Muntean, A., Pop, I.S., Suciu, N., Kolditz, O.: A mixed finite element discretization scheme for a concrete carbonation model with concentration-dependent porosity. J. Comput. Appl. Math. **246**, 74–85 (2013)
26. Chalupecky, V., Fatima, T., Muntean, A., Kruschwitz, J.: Macroscopic corrosion front computations of sulfate attack in sewer pipes based on a micro-macro reaction-diffusion model. In Multiscale Mathematics: Hierarchy of collective phenomena and interrelations between hierarchical structures (Fukuoka, Japan, December 8–11, 2011). COE Lecture Note Series, vol. 39 pp. 22–31. Fukuoka: Institute of Mathematics for Industry, Kyushu University (2012)
27. Klöfkorn, R., Kröner, D., Ohlberger, M.: Local adaptive methods for convection dominated problems. In: ICFD Conference on Numerical Methods for Fluid Dynamics (Oxford, 2001) Int. J. Numer. Methods Fluids **40**(1–2):79–91 (2002)
28. Ohlberger, M., Rohde, C.: Adaptive finite volume approximations for weakly coupled convection dominated parabolic systems. IMA J. Numer. Anal. **22**(2), 253–280 (2002)
29. Cariaga, E., Concha, F., Pop, I.S., Sepúlveda, M.: Convergence analysis of a vertex-centered finite volume scheme for a copper heap leaching model. Math. Methods Appl. Sci. **33**(9), 1059–1077 (2010)
30. Rivière B., Wheeler, M.F.: Non conforming methods for transport with nonlinear reaction. In: Fluid flow and transport in porous media: mathematical and numerical treatment (South Hadley, MA, 2001). Contemp. Math., vol. 295, pp. 421–432. American Mathematical Society, Providence (2002)
31. Dawson, C.: Analysis of an upwind-mixed finite element method for nonlinear contaminant transport equations. SIAM J. Numer. Anal. **35**(5), 1709–1724 (1998)
32. Dawson, C., Aizinger, V.: Upwind-mixed methods for transport equations. Comput. Geosci. **3**(2), 93–110 (1999)
33. Eymard, R., Hilhorst, D., Vohralík, M.: A combined finite volume-nonconforming/mixed-hybrid finite element scheme for degenerate parabolic problems. Numer. Math. **105**(1), 73–131 (2006)
34. Hilhorst, D., Vohralík, M.: A posteriori error estimates for combined finite volume-finite element discretizations of reactive transport equations on nonmatching grids. Comput. Methods Appl. Mech. Eng. **200**(5–8), 597–613 (2011)
35. Ciavaldini, J.F.: Analyse numerique d'un problème de Stefan à deux phases par une methode d'éléments finis. SIAM J. Numer. Anal. **12**, 464–487 (1975)
36. Kumar, K., Pop, I.S., Radu, F.A.: Convergence analysis of mixed numerical schemes for reactive in a porous medium. SIAM J. Numer. Anal. **51**, 2283–2308 (2013)
37. Devigne, V.M., Pop, I.S., van Duijn, C.J., Clopeau, T.: A numerical scheme for the pore-scale simulation of crystal dissolution and precipitation in porous media. SIAM J. Numer. Anal. **46**(2), 895–919 (2008)
38. Mikelić, A., Devigne, V., van Duijn, C.J.: Rigorous upscaling of the reactive flow through a pore, under dominant Peclet and Damkohler numbers. SIAM J. Math. Anal. **38**, 1262–1287 (2006)
39. Girault, V., Riviere, B., Wheeler, M.F.: A splitting method using discontinuous galerkin for the transient incompressible Navier–Stokes equations. ESAIM: M2AN **39**(6):1115–1147 (2005)
40. Knobloch, P., Tobiska, L.: On the stability of finite-element discretizations of convection–diffusion-reaction equations. IMA J. Numer. Anal. **31**(1), 147–164 (2011)
41. van Noorden, T.L., Pop, I.S, Röger, M.: Crystal dissolution and precipitation in porous media: L^1-contraction and uniqueness. Discrete Contin. Dyn. Syst., (Dynamical Systems and Differential Equations. Proceedings of the 6th AIMS International Conference, suppl.), 1013–1020 (2007)

42. Ciarlet, P.G.: The finite element method for elliptic problems. In: Studies in Mathematics and its Applications, vol. 4. North-Holland Publishing Co., Amsterdam (1978)
43. Ladyzhenskaya, O.A., Ural'tseva, N.N.: Linear and quasilinear elliptic equations. Academic Press, New York (1968) (Translated from the Russian by Scripta Technica, Inc. Translation editor: Leon Ehrenpreis)
44. Simon, J.: Compact sets in the space $L^p(0, T; B)$. Ann. Mat. Pura Appl. **146**(4), 65–96 (1987)
45. Brezis, H.: Functional Analysis. In: Sobolev Spaces and Partial Differential Equations. Springer, New York (2011)
46. Lenzinger, M., Schweizer, B.: Two-phase flow equations with outflow boundary conditions in the hydrophobic–hydrophilic case. Nonlinear Anal. **73**(4), 840–853 (2010)
47. Temam, R.: Navier–Stokes equations. In: Studies in Mathematics and its Applications, vol. 2, 3rd edn. North-Holland Publishing Co., Amsterdam (1984) (Theory and numerical analysis. With an appendix by F, Thomasset)
48. Pop, I.S., Radu, F., Knabner, P.: Mixed finite elements for the Richards' equation: linearization procedure. J. Comput. Appl. Math. **168**(1–2), 365–373 (2004)
49. Elliott, C.M.: Error analysis of the enthalpy method for the Stefan problem. IMA J. Numer. Anal. **7**(1), 61–71 (1987)